THE UNIVERSITY of EDINBURGH

Edinburgh Research Explorer

Diamond formation in the deep mantle: the record of mineral inclusions and their distribution in relation to mantle dehydration zones

Citation for published version:
Harte, B 2010, 'Diamond formation in the deep mantle: the record of mineral inclusions and their distribution in relation to mantle dehydration zones', *Mineralogical Magazine*, vol. 74, no. 2, pp. 189-215. https://doi.org/10.1180/minmag.2010.074.2.189

Digital Object Identifier (DOI):
10.1180/minmag.2010.074.2.189

Link:
Link to publication record in Edinburgh Research Explorer

Document Version:
Publisher's PDF, also known as Version of record

Published In:
Mineralogical Magazine

Publisher Rights Statement:
Published in an issue of Mineralogical Magazine by the Mineralogical Society (2010)

General rights
Copyright for the publications made accessible via the Edinburgh Research Explorer is retained by the author(s) and / or other copyright owners and it is a condition of accessing these publications that users recognise and abide by the legal requirements associated with these rights.

Take down policy
The University of Edinburgh has made every reasonable effort to ensure that Edinburgh Research Explorer content complies with UK legislation. If you believe that the public display of this file breaches copyright please contact openaccess@ed.ac.uk providing details, and we will remove access to the work immediately and investigate your claim.

OPEN ACCESS

Download date: 12. Oct. 2024

Mineralogical Magazine, April 2010, Vol. 74(2), pp. 189–215

Review

Diamond formation in the deep mantle: the record of mineral inclusions and their distribution in relation to mantle dehydration zones

B. Harte*

Grant Institute of Earth Sciences, School of Geosciences, University of Edinburgh, Edinburgh EH9 3JW, UK

[*Received 15 November 2009; Accepted 30 March 2010*]

ABSTRACT

Studies of the inclusions contained in natural diamonds have shown the occurrence of minerals which must have formed at depths below the lithosphere and which may be closely matched with the silicate mineral assemblages determined by high pressure and temperature experimental studies for depths of 300 to 800 km in the Earth's mantle. The inclusions come principally from two main depth zones: (1) the lower asthenosphere and upper transition zone; (2) the Upper Mantle/Lower Mantle (UM/LM) boundary region and the uppermost LM. The inclusions from zone 1 are very largely majoritic garnets (with or without clinopyroxene) which indicate bulk compositions of eclogitic/metabasic affinity. The minerals from zone 2 include Ca-Si and Mg-Si perovskites and ferropericlase and are dominantly of metaperidotitic bulk composition, but include some possible metabasite assemblages. In many of these natural assemblages, the tetragonal almandine pyrope phase occurs rather than the garnet found in experiments.

As natural diamonds are believed to crystallize in fluids/melts, the hypothesis is developed that the restriction of diamonds and inclusions of particular compositions to the above two depth intervals is because they are controlled by loci of fluid/melt occurrence. Attention is focused on subduction zones because both suites of inclusions show some evidence of subducted protoliths. The lower zone (600–800 km) coincides with the region where dehydration may be expected for hydrous ringwoodite and dense hydrous Mg-silicates formed in subducted peridotites. The dehydration of lawsonite in subducted metabasites provides a particular location for melt formation and the inclusion of the shallower (~300 km) majoritic inclusions. For the deeper majoritic inclusions in the region of the upper transition zone, melt development may occur as a consequence of the hydrous wadsleyite-to-olivine transformation, and such melt may then interact with the upper crustal portion of a subducting slab. These suggestions offer an explanation of the depth restrictions and the compositional restrictions of the inclusions. The differences in $\delta^{13}C$ values in the host diamonds for the two suites of inclusions may also be explained on this basis.

Keywords: majoritic garnet, Ca-Si perovskite, Mg-Si perovskite, hydrous wadsleyite, hydrous ringwoodite, dense hydrous Mg-silicates, dehydration reactions.

Introduction and background

This paper considers the provenance of mineral inclusions found in natural diamonds which appear to come from below the Earth's lithosphere. Attention will be focused on the inclusions which appear to come from ultrabasic and basic bulk rock compositions. Comparison of these inclusions with experimental data shows that they have selective distributions with respect to depth: with basic ones coming predominantly from a region in the lower asthenosphere and upper transition zone, and ultrabasic ones from a region spanning the base of the transition zone

* E-mail: ben.harte@ed.ac.uk
DOI: 10.1180/minmag.2010.074.2.189

© 2010 The Mineralogical Society

(TZ) and the uppermost lower mantle. The hypothesis will be developed that this distribution is controlled by the occurrence of dehydration and generation of fluids/melts which form the locations of diamond growth. For the inclusions of ultrabasic affinities, the dehydration is linked to reactions involving dense hydrous Mg-silicates (DHMS) and hydrous ringwoodite in cool subducted slabs (Komabayashi, 2006). For inclusions of basic affinity, the situation is less clear, but links to dehydration of lawsonite in subducted metabasites are suggested in conjunction with potential interaction with melts formed from the dehydration of hydrous wadsleyite to olivine (e.g. Kawamoto, 2006; Karato, 2006).

Overall, a huge amount of research by both mineralogists and physicists has been carried out on diamonds, inclusions in diamonds, and on mantle xenoliths formed in the diamond stability field in the lower continental mantle lithosphere. Reviews of such research may be found for example in Harris (1987), Gurney (1989), Harte and Hawkesworth (1989), Pearson *et al.* (2003) and Stachel and Harris (2008). In the following introductory notes, I summarize some key points of this extensive previous research. Although most of these observations have been based primarily on research into lithospheric diamonds, they are generally believed to be applicable also to sublithospheric diamonds, and therefore constitute pertinent background to this paper.

General features of natural diamonds

(1) On the basis of morphology and internal growth structures, natural diamonds are normally believed to crystallize in the mantle from fluids rather than in the solid state. These fluids might vary from C-O-H-rich to carbonatitic and silicate-rich melts. Since diamond stability commonly demands formation at pressures in excess of 4.5 to 5 GPa (~150 km depth), fluids of these compositions will show considerable miscibility with one another (Kawamoto, 2006; Litvin *et al.*, 2008). The actual precipitation of diamonds from fluid/melt is commonly believed to be caused by reduction/oxidation events (e.g. Deines, 1980; Haggerty, 1986; Taylor and Green, 1989), and this has also been proposed for 'deep' diamonds (e.g. Stachel, 2001; Bulanova *et al.*, 2010).

(2) The syngenetic mineral inclusions trapped in diamonds often show evidence of an imposed morphology with crystal surfaces parallel to diamond crystal faces, and this is believed to indicate simultaneous growth of the inclusion and the diamond (e.g. Harris and Gurney, 1979). Thus the conditions of formation of inclusion and host diamond are the same.

(3) Once trapped inside diamond, the inclusions are protected from the medium surrounding the diamond, and are therefore believed to maintain constant chemical composition. However, changes in temperature and pressure may cause instability of included minerals and replacement by other phases even though the bulk chemistry remains constant.

(4) The ages found for formation of lithospheric diamonds, typically based on radiometric dating of inclusions, are commonly Archaean and Proterozoic, whilst the eruption ages of the kimberlites bringing diamonds to the surface are mainly Phanerozoic (e.g. Shirey *et al.*, 2004 and references therein). Thus, diamonds are typically much older than their eruption age, and the tectonic setting of their formation may be very different from that of their eruption towards the Earth's surface. For the diamonds with ultrabasic and basic inclusions considered here, definite age data are lacking, but it is important to stress the general point that the age of kimberlite eruption is unlikely to be the age of diamond formation.

The spectrum of inclusions in diamonds

(a) The mineral inclusions found within diamonds are mostly silicates, but also include oxides, sulphides and rarely carbonates. Of these, the silicates are by far the easiest to relate to particular conditions of formation at depth within the mantle, because of the extensive high-pressure experimental work done on silicate compositions.

(b) The great majority of silicate minerals found as inclusions in diamonds are typical of those expected, and known to occur, in ultrabasic and basic rocks forming deep continental lithosphere (up to depths of ~210 km and bordering on the asthenosphere). Typically, they fall into two major groups with minerals similar to those seen in peridotites (ultrabasic) and in eclogites (basic) recovered as xenoliths from mantle lithosphere. Occasionally, included mineral compositions fall between the typical peridotitic and eclogitic compositions, and these are usually referred to as websteritic.

(c) The 'deep mantle silicate' inclusions under discussion here are rare and show new phases and new phase compositions compared with those of

TABLE 1. List of mineral phases and abbreviations.

ak	akimotoite
atg	antigorite
CaTiPvk	Ca-Ti perovskite ('normal' perovskite)
cf	Na-Ca-Mg-Al-Si phase with calcium ferrite structure
chr	chromite
cpv	Ca-Si perovskite
cpx	clinopyroxene
DHMS	dense hydrous Mg-silicates
en	enstatite
fl	fluid/melt
fPer	ferropericlase
fo	fosterite
grt	garnet
hpA	hydrous-phase A
hpD	hydrous-phase D
hy-rw	hydrous ringwoodite
hy-wd	hydrous wadsleyite
LM	lower mantle
lws	lawsonite
maj	majoritic garnet
mpv	Mg-Si perovskite
mpv (Al)	Mg-Si perovskite (Al-rich)
NAL	Na- and Al-bearing phase
ol	olivine
opx	orthopyroxene
rw	ringwoodite
shpB	super-hydrous-phase B
stv	stishovite
TAPP	tetragonal almandine pyrope phase
ttn	titanite
TZ	transition zone
UM	upper mantle
UM/LM boundary	upper mantle/lower mantle boundary
wd	wadsleyite

the lithosphere (see Table 1 for a listing of phases and abbreviations). These include Mg-Si perovskite (mpv) and Ca-Si perovskite (cpv) with Si in sixfold coordination, and for convenience these will be referred to as 'silicates' as well as the usual silicates showing fourfold coordination. For the most part, all phases may again be referred to bulk rock compositions of ultrabasic and basic character, but the mineral assemblages change several times with depth and the rocks represented cease to be peridotites and eclogites from the mineralogical and petrographic viewpoint. To avoid new names, I adopt the simple option from metamorphic petrology of referring collectively to these two rock groups as 'metaperidotites' and 'metabasites'. The term metabasite is preferred to meta-eclogite or indeed metabasalt, because I do not wish to imply that the initial mineralogy was necessarily either that of a basalt or an eclogite. Peridotites on the other hand have much wider stability fields and are taken to include rocks formed from model geochemical compositions such as pyrolite (Ringwood, 1991).

Although this paper focuses on the common ultrabasic (metaperidotite) and basic (metabasite) inclusion suites and their relation to experimental data on silicate assemblages, some notes will also be made on unusual inclusions, such as those involving carbonate and others with Ca-Ti-silicates (Brenker *et al.*, 2005, 2007; Walter *et al.*, 2008; Bulanova *et al.*, 2010) which indicate special protoliths and conditions of formation.

Sources of diamonds with sublithospheric mineral inclusions

Although relatively rare, compared to lithospheric minerals, inclusions of minerals with sublithospheric characteristics have now been recorded from a wide variety of localities for diamonds of both *in situ* kimberlite and alluvial sources. Typically, diamonds are associated with the stable, tectonically quiescent, domains of cratons (Dawson, 1989). Figure 1 highlights specific localities within four cratons (Kalahari in southern Africa, Guapore in Brazil, west Africa, and the Slave craton in Canada) where relatively large numbers of diamonds with deep mantle inclusions have been found. But it must be noted that other localities occur throughout the world where occasional deep-mantle diamonds have been reported and these include Yakutia, the Sino-Korean craton and the South Australia craton.

Experimental data on expected mantle mineral assemblages in the depth region 300–800 km

On the basis of extensive seismological and density studies of the Earth, coupled with chemical composition constraints based on petrology and geochemistry in the Earth and Solar System, the mantle is considered to be formed largely by rock compositions falling into the same two major groups as those commonly found for diamond inclusions and mantle xenoliths, i.e. ultrabasic compositions (represented by peridotite and metaperidotite rocks) and basic compositions (represented by basalts and eclogites and metabasites in broad terms).

Both rock compositions, and related simplified systems (with fewer chemical components) have been the subject of extensive experimental work to determine the likely minerals and mineral assemblages present in the mantle. Particular average or model bulk compositions of these two groups are often used to estimate proportions of minerals present in these bulk compositions at particular depths and to estimate properties such as seismic velocity and density. The average bulk compositions used for peridotites are usually based on the pyrolite model of Ringwood (1991) or on the depleted MORB mantle of Workman and Hart (2005), both of which give similar results. For basaltic rock bulk compositions, average MORB basalt is commonly used. Discussions of mineral compositions and proportions with depth are given, for example, by Irifune and Ringwood (1987) and Fei and Bertka (1999). Figure 2 shows minerals and mineral proportions for both model bulk compositions based on recent papers by Stixrude and Lithgow-Bertelloni (2007) and Perillat *et al.* (2006).

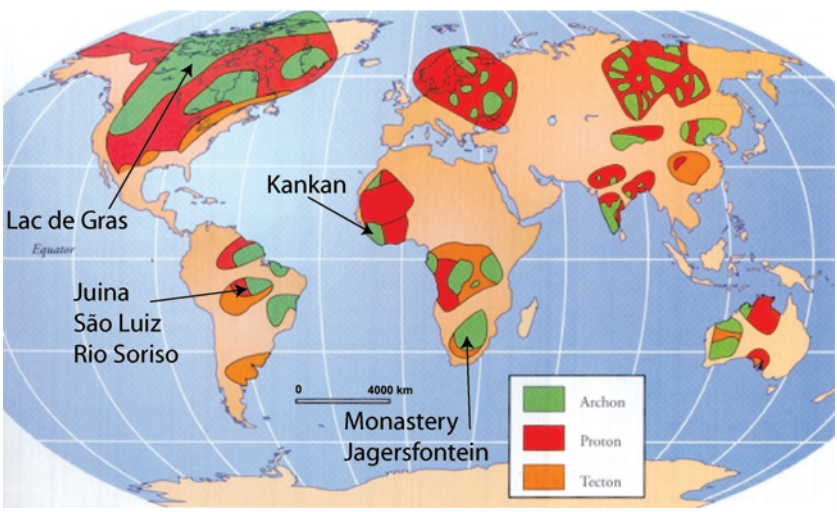

FIG. 1. Worldwide distribution of cratons and the locations of principal sources of diamonds containing inclusions of sublithospheric origin. The relative ages of the cratons are: Archons – >2.5 Ga; Protons – 1.6 to 2.5 Ga; Tectons – 0.8 to 1.6 Ga. Adapted from Harlow and Davies (2005).

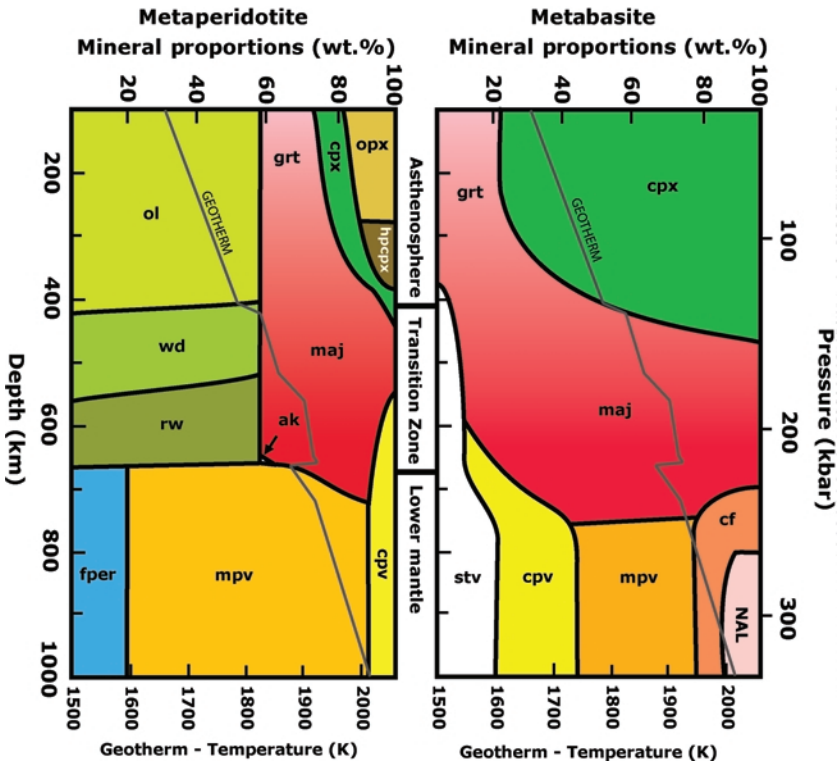

FIG. 2. Mineral proportions present in average metaperidotite and metabasite bulk compositions as a function of depth ranging from 100–1000 km, adapted from Stixrude and Lithgow-Bertelloni (2007), and Perrillat *et al*. (2006). The geotherm, giving temperatures as a function of depth is also from Stixrude and Lithgow-Bertelloni (2007).

The metaperidotite at the shallowest level in Fig. 2 has the typical mineral assemblage (olivine, garnet, orthopyroxene, clinopyroxene) of garnet-peridotite xenoliths derived from the continental mantle lithosphere. With increasing depth, the dominant $(Mg,Fe)_2SiO_4$ phase changes from olivine (ol) to wadsleyite (wd) and then ringwoodite (rw). At the UM/LM boundary, ringwoodite ceases to be stable and is replaced by ferropericlase (fPer) and mpv in the reaction:

$$(Mg,Fe)_2SiO_4 = (Mg,Fe)O + (Mg,Fe)SiO_3$$

The wd and rw phases dominate the TZ which coincides with well recognized seismic discontinuities. It forms the lower part of the upper mantle (UM), with its base coinciding with the UM/LM boundary. We shall refer to that part of the UM above the TZ as the asthenosphere (Fig. 2), or the convecting uppermost mantle, as distinct from the UM at the highest level which forms the lithosphere. The depth locations of the upper and lower boundaries of the TZ do not appear to be strongly affected by reasonable variations in temperature or Fe-Mg composition or the potential presence of H or H_2O in the wd and rw compositions (e.g. Karato, 2006).

The dominant additional phase in metaperidotite compositions in the UM is garnet, which increases in abundance with depth (Fig. 2) as orthopyroxene and clinopyroxene pass effectively into solid solution within the garnet to give the special variety of garnet compositions containing majorite end-member components (see Ringwood and Major, 1971). In the upper part of the TZ, majoritic garnets embrace a wide range of Mg-Fe-Ca compositions, but in the lower part of the TZ, cpv becomes stable and becomes the dominant Ca-bearing phase with passage into the lower mantle (LM). Within the LM, mpv widens its composition field to take Al into solid solution and as a result, with increasing depth, metaperidotite bulk compositions (with limited total Al

content) soon cease to carry a pyrope-rich garnet or majoritic garnet as the dominant Al-bearing phase (Fig. 2).

In metabasite compositions, the changes in mineral assemblage occurring with depth are similar to those affecting the garnet + pyroxene components of metaperidotites. The dominant metabasite assemblage of the upper part of the convecting mantle (asthenosphere) is eclogite (garnet + clinopyroxene), and with increasing depth, garnet undergoes a similar expansion of its composition range to that seen in metaperidotite assemblages. In metabasite rocks in the TZ this means that majoritic garnet will commonly form >80% of the rock. With increasing depth, first the Ca components of majoritic garnet give rise to cpv then the Mg-Fe components form mpv. Again, Al goes into mpv as depth increases in the LM, but because of the larger Al contents of metabasite compositions, garnet (now with decreasing majorite content) persists to greater depths than in metaperidotites (Fig. 2). In addition, the larger Na as well as the Al contents of metabasite compositions result in the formation of additional phases such as the Na- and Al-bearing phase (NAL) and Na-Ca-Mg-Al-Si phase (cf) listed in Table 1 and documented by Hirose and Fei (2002) and Perillat *et al.* (2006).

Depth zones indicated by inclusions in deep diamonds

The minerals found as inclusions in diamonds, on the basis of experimental work, show many of the mineralogical changes shown in Fig. 2. In many cases, the inclusions found in diamonds are single minerals, but several inclusions of different minerals may occur in one diamond. Usually, the inclusions within one diamond appear to be compatible with one another, but cases have been reported where several minerals in one diamond are clearly out of equilibrium with one another. Therefore, at the outset, I refer to sets of inclusions in the same diamond as mineral associations rather than mineral assemblages (Harte *et al.*, 1999*b*).

In comparing the natural minerals and their associations with the experimentally based mineralogy of Fig. 2, it is useful to classify the minerals and their assemblages into groups according to depth. Thus, we may recognize a series of major depth zones or metamorphic facies (Eskola, 1920), each facies being characterized by particular mineral assemblages. Such subdivision might be done in detail for precise changes in mineral assemblages and/or mineral compositions for very specific bulk compositions, but the objective here is to emphasize the major changes seen in Fig. 2. Therefore, a schematic series of broad depth zones or facies subdivisions is recognized for both metaperidotite and metabasite rock compositions. These are shown in Table 2 together with the model mineral assemblages for both metaperidotite and metabasite bulk-rock compositions as summarized in Fig. 2. Whilst the positions in depth for several changes in metaperidotite and metabasite mineral assemblages are broadly similar, this is not true at the UM/LM boundary. At this depth, metaperidotite undergoes the sharp transition to fPer+mpv assemblages in the place of ringwoodite; whilst in metabasites there is only a gradual contraction in majorite stability, and mpv only becomes the dominant phase once it can accommodate significant Al. This difference at the UM/LM boundary, and the resultant differences in density changes for metaperidotite and metabasite rocks, has been an important factor in the development of ideas concerning subduction-slab pile-ups and megalith formation at the UM/LM boundary (e.g. Irifune and Ringwood, 1987; Ringwood, 1991). We shall return to these concepts in the Discussion section.

The detailed comparison of minerals and their associations found as inclusions within diamonds with experimentally-based facies or depth zones is summarized in Table 2. However, an additional zone has been added in Table 2. Because several sets of inclusion mineral associations appear to come from the actual UM/LM boundary (e.g. Hutchison *et al.*, 2001; Stachel *et al.*, 2005; Hayman *et al.*, 2005), a zone of UM/LM boundary associations has been placed in the list of depth zones, and the apparent abundance of inclusions from this narrow depth will be discussed at some length below.

There is one major exception to the close comparison of experimentally predicted phases and natural minerals found. In the lower part of the TZ and uppermost LM, majoritic garnets are essentially replaced by a tetragonal almandine-pyrope phase (TAPP). This phase has compositions which could be represented in terms of almandine + pyrope garnet components, but it has a different atomic structure to garnet (Harris *et al.*, 1997). Various interpretations of its occurrence have been debated (e.g. Harte *et al.*, 1999*b*), but it now seems most likely that it is stabilized by its

TABLE 2. Simplified sequence of major mineral assemblages and inclusion associations in diamond with depth.

Metaperidotites			Metabasites		
Depth zone/facies	Model rock mineral assemblage[1]	Principal inclusions in diamonds[2,3]	Depth zone/facies	Model rock mineral assemblage[1]	Principal inclusions in diamonds[2,3]
Grt peridotite	ol+opx+cpx+grt	ol, opx, grt, [cpx, chr][4]	Eclogite	cpx+grt	grt, cpx [SiO_2, kyanite][4]
Maj peridotite	ol+maj (cpx)	?	Cpx-majorite	maj+cpx	maj, cpx[5]
Maj 'wd-peridotite'	wd+maj	?	Majorite	maj+stv	maj
Maj 'rw-peridotite'	rw+maj (cpv)	?	Cpv-majorite	maj+cpv+stv	?
Upper/Lower Mantle Boundary association	rw+mpv+fper+ maj+cpv	Mg_2SiO_4, mpv, fPer, tapp, cpv	UM/LM boundary association	maj+cpv+stv	maj(NaAlPx or NaPx)[6], tapp,
Ferropericlase and MgSi-perovskite (Al-poor)	mpv+fPer+ maj+cpv	mpv, fPer, tapp, cpv	Cpv-majorite	maj+cpv+stv	tapp, cpv, [stv]
Ferropericlase and MgSi-perovskite (Al-rich)	mpv(Al)+ fPer+cpv	mpv(Al)[7], fPer, cpv	MgSi-perovskite (Al-rich) and cpv	mpv(Al)[7]+cpv+stv	mpv(Al)[7], cpv, [crn] [stv][4]

[1] Assemblages based on Fig. 2.
[2] The inclusions in diamonds are often single minerals and are therefore listed separately. Associations of several inclusions in one diamond are listed in Table 4 and discussed in text. The identification of inclusions has often been based on chemical composition alone.
[3] Inclusions listed are restricted to silicates, with the exception of fPer and chr. For inclusion associations involving only oxides see Kaminsky *et al*. (2001, 2009). SiO_2 is only listed where found with other silicates. SiO_2 inclusions occurring alone or with fPer may show evidence of disequilibrium (Stachel *et al*., 2000*b*; Hayman *et al*., 2005).
[4] Phases in square brackets are of limited occurrence or abundance.
[5] Often the clinopyroxene occurs in the same inclusion as majoritic garnet and is probably formed by exsolution from a higher pressure majorite solid solution (Harte and Cayzer, 2007).
[6] These are rarely reported pyroxene phases with high Na or Na+Al, which are believed to have initially crystallized with garnet structure probably in association with cpv and melt (Gasparik and Hutchison, 2000; Hutchison *et al*., 2001).
[7] In this Table 'mpv(Al)' refers to high-Al MgSi-perovskite (with >4 wt. % Al_2O_3), whereas 'mpv' refers to low-Al MgSi-perovskite. At the UM/LM boundary, ak may occur in place of mpv (Fig. 2).

capacity to hold Fe^{3+} which is relatively abundant in deep mantle silicates (e.g. McCammon *et al.*, 2004; Frost *et al.*, 2004). An association of fPer and mpv in diamond, and a TAPP inclusion are illustrated in Fig. 3*c* and 3*d*.

So far, the NAL and cf silicate phases (Table 1) found in experimental metabasite compositions (Fig. 2) have not been identified in inclusion associations, but it is possible that the inclusion-bearing diamonds do not normally come from sufficient depths (see later Discussion).

Although the inclusion phases generally show a correspondence with experimental mineral assemblages, the inclusion mineral sample is far from being a random sample of all depth zones for each of the two major bulk compositions. If we exclude the metaperidotite mineral associations of the uppermost UM and the UM/LM boundary, there is an absence of metaperidotite associations for the greater part of the UM (Table 2). Likewise, there is only minimal evidence on the occurrence of metabasite associations from the central and deeper region of the TZ. Thus, two depth intervals predominate in providing the great majority of deep mantle inclusions:

(1) the lower asthenosphere and the upper TZ, where the inclusions are of metabasite affinity (cpx-majorite and majorite facies in Table 2);

(2) the lowermost TZ and the uppermost part of the LM (the three deepest depth zones in

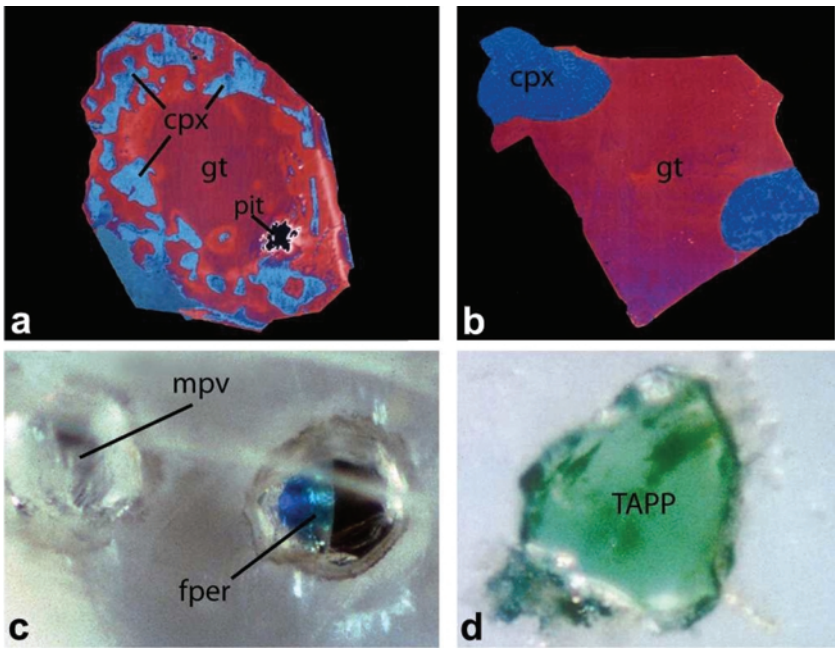

FIG. 3. Images of deep mantle inclusions in diamonds. (*a*) and (*b*) BSE images showing two majorite-eclogite inclusions (150–200 μm) after break-out from their host diamonds. The intensity of the backscattered signal has been converted to a blue-red scale so that clinopyroxene appears blue and garnet (both with and without a majoritic component) appears in magenta to red colours. (*a*) Inclusion BZ43 with extensive areas of omphacitic clinopyroxene in the outer part of the inclusion; the garnet in the central area is darker coloured (and has a high majorite component) compared to the usually redder (and more normal Si) garnet adjacent to clinopyroxene. Note that despite a generally irregular appearance, some of the edges of the clinopyroxenes have straight segments with common orientations and are believed to result from exsolution from original very Si-rich majorite. (*b*) Inclusion BZ20 has homogenous normal-Si garnet and omphacitic clinopyroxene in smooth-edged grains (slight variations in colour result from polishing). The sharp kink in the garnet-clinopyroxene boundary in the top left coincides with a grain boundary within the clinopyroxene. This 'eclogite' inclusion is believed to have formed by recrystallization from an original majoritic garnet (Harte and Cayzer, 2007). (*c*) and (*d*) Photographs of inclusions (40–50 μm) within diamonds. (*c*) Shows a fPer with iridescent blue effect on a polished surface together with a colourless perovskite (probably mpv) lying below the surface. (*d*) TAPP.

Table 2), where the inclusion associations often include fPer and are dominantly of metaperidotite affinity, although some metabasite associations are also recognized.

The differences in overall bulk composition of inclusions in those two suites are also notable and we shall discuss each suite in turn.

Inclusions of metabasite affinity from the uppermost TZ and asthenosphere

Nearly all the majoritic garnets found as inclusions in diamonds are of metabasic affinity, with bulk compositions clearly related to those of lower-pressure (eclogitic) garnets in being relatively Ca-rich, poor in Cr, and with a relatively high Fe/(Fe+Mg) ratio. The exceptions have large to very large Cr_2O_3 contents, indicating websteritic and peridotitic bulk compositions, and are thought to be derived from exceptionally thick lithosphere (Stachel, 2001; Pokhilenko *et al.*, 2004; Stachel *et al.*, 2005). At some localities, the Cr-rich majorites are accompanied by Cr-poor garnets of weakly majoritic affinity. This situation is well illustrated by the inclusions from Snap Lake/King Lake (Slave, Canada) where two weakly majoritic basic inclusions occur alongside majorites of ultrabasic

compositions whose Cr_2O_3-rich nature suggests derivation from particularly thick (up to ~300 km deep) lithosphere (Pokhilenko *et al.*, 2004). Similar situations, where the dominant majoritic garnets are distinctly Cr-bearing and indicative of peridotitic and/or websteritic bulk compositions, are seen at Premier (Gurney *et al.*, 1985), Arkhangelsk (Sobolev *et al.*, 1997), Yakutia (Sobolev *et al.*, 2004) and Wawa (Stachel *et al.*, 2006). The majoritic garnets from these localities are therefore omitted from further consideration, on the basis that they probably derive from particularly thick lithosphere and may well be distinct from the dominant metabasic majorites which commonly imply depths of origin below 300 km.

Table 3 summarizes the worldwide occurrences of metabasic garnet inclusions with a majoritic component. Following Tappert *et al.* (2005*a*), any garnets with more than 3.05 Si per 12 oxygens p.f.u. have been taken as being 'majoritic'. Inclusions of majoritic garnet were first reported by Moore and Gurney (1985) from the Monastery mine, S. Africa, with EMPA analyses showing Si contents well in excess of 3 Si a.p.f.u. per 12 oxygens. Later descriptions of the Monastery inclusions noted, in some cases, the occurrence of clinopyroxene with majoritic garnet (Moore and Gurney, 1989; Moore *et al.*, 1991). Wilding (1990) documented majorite-bearing inclusions from São Luiz (Brazil) and noted the common occurrence of clinopyroxene alongside majorite in the same inclusion. Further studies (Harte, 1992; Harte and Cayzer, 2007), with improved BSE and EBSD imaging, found omphacitic clinopyroxene occurring alongside majorite in all the São Luiz inclusions, in many cases the garnets showing variable composition and complex textures (Fig. 3*a*), suggesting exsolution. Clinopyroxene occurs with majoritic garnet in two out of three diamonds at Kankan (Stachel *et al.*, 2000*a*), and in one out of two diamonds at Buffalo Hills (Davies *et al.*, 2004*b*). At many of the localities where very few diamonds have yielded majoritic inclusions, it is not unusual for several inclusions in one diamond to show varying compositions and, in some cases, for compositional variations in one inclusion to indicate exsolution of clinopyroxene from majorite (e.g. Kaminsky *et al.*, 2001).

The detailed textural and compositional relationships of garnet and clinopyroxene in inclusions of this type (Fig. 3*a*,*b*) were particularly investigated by Harte and Cayzer (2007), who found that the majoritic garnets from São Luiz were typically single crystals with intergrowths of omphacitic clinopyroxene, whose preferred crystallographic orientation indicated an exsolution origin. The extent of exsolution was shown to vary and gave rise to garnet compositions that had variable majorite content within a single inclusion (Fig. 3*a*). In other inclusions from São Luiz, garnet without a majorite component occurred alongside omphacitic clinopyroxene (Fig. 3*b*), with both minerals showing compositions typical of eclogitic assemblages from the mantle lithosphere. The close similarities of bulk compositions in both majorite-bearing inclusions and non-majorite-bearing inclusions suggested to Harte and Cayzer (2007) the possibility that all inclusions had a similar origin, but had undergone variable amounts of clinopyroxene exsolution and recrystallization. A similar occurrence of majorite-bearing inclusions and garnet + clinopyroxene inclusions was also noted for the sets of inclusions from Monastery, and led Moore *et al.* (1991) to suggest that both sets of inclusions may have had a common origin. However, evidence of decompression and exsolution of original majorite single-phase inclusions is not found in the case of the Jagersfontein inclusions where clinopyroxene is not recorded (Tappert *et al.*, 2005*a*).

A plot of majoritic garnet compositions is shown in Fig. 4. The typical metabasite garnets of the Earth's crust and uppermost mantle have compositions of the form $\{X^{2+}\}_3[Y^{3+}]_2(Si)_3O_{12}$, in which: $\{X\}$ are divalent cations (commonly Fe^{2+}, Mg^{2+}, Mn^{2+}, Ca^{2+}) in distorted eightfold coordinated sites; $[Y]$ are trivalent cations (most commonly Al^{3+}, Cr^{3+} and Fe^{3+}) and also, most likely, Ti^{4+} in sixfold coordinated sites; the Si^{4+} is in fourfold coordination and, in eclogitic garnets, is characteristically constrained to 3 cations per 12 oxygens. In the case of higher pressure, majoritic garnets, Si^{4+} occurs on the sixfold Y site as well as occupying the fourfold site and consequently Si^{4+} exceeds 3 cations p.f.u. This is illustrated in Fig. 4*a*, where increasing Si cations >3.0 are associated with a decline of the Y site cations (R^{3+} + Ti^{4+}). Where Si^{4+} substitutes for R^{3+} cations on the Y site, the charge balance may be maintained in two principal ways:

(i) monovalent Na^+ substitutes for divalent cations on the X site – $R^{3+} + R^{2+} = Si^{4+} + Na^+$;

(ii) a divalent cation substitutes for a trivalent cation on the Y site – $2R^{3+} = Si^{4+} + R^{2+}$.

In the first case, one Si^{4+} is balanced by the loss of one R^{3+} on the Y site (shown as idealized trend

TABLE 3. Principal localities of majoritic garnet inclusions of metabasic/eclogitic composition.

Locality	Craton	No. of diamonds with majorite inclusionss	No. of diamonds with both majorite and clinoyroxene	Majorite compositional range Si^{4+} p.f.u. (O = 12)	*P* range* (Gpa)	$\delta^{13}C$‰** Diamond host	References
Monastery	Kalahari	46	3	3.070–3.335	7.5–14.0		Moore and Gurney (1985, 1989); Moore *et al.* (1991)
São Luiz	Guapore	17	17	3.050–3.381	7.5–14.5	−4.6 to −11.0	Wilding (1990); Hutchison (1997); Harte and Cayzer (2007)
Jagersfontein	Kalahari	13	0	3.078–3.542	8.5–16.0	−17.2 to −24.0	Tappert *et al.* (2005); Deines *et al.* (1991)
Kankan	West Africa	3	2	3.116–3.279	10.0–13.5	0.89 to −3.1	Stachel *et al.* (2000*a*, 2002)
Buffalo Hills	Buffalo Head Terrane	2	1	3.122–3.188	11.0–12.0	−4.8 to −14.8	Davies *et al.* (2004*b*)
Mwadui	Central Africa	1	0	3.090	9.0	−11.5	Stachel *et al.* (1998)
DO-27	Slave	2	1	3.170	12.0	−13.4 to −17.0	Davies *et al.* (1999)
Juina	Guapore	2	1	3.051–3.118	7.5–10.5	−13.3 to −7.5	Kaminsky *et al.* (2001); Bulanova *et al.* (2010)

* Pressure estimates are based on the Si contents determined in experiments by Akaogi and Akimoto (1979) and Irifune (1987); the calibrations probably have uncertainties of at least ±1.5 GPa (see text).
** The carbon isotope compositions of the host diamonds are usually available for only a subset of the inclusions investigated.
Localities where the principal majoritic garnets indicate ultrabasic bulk compositions, probably indicating derivation from exceptionally thick lithosphere, have been omitted (see text).

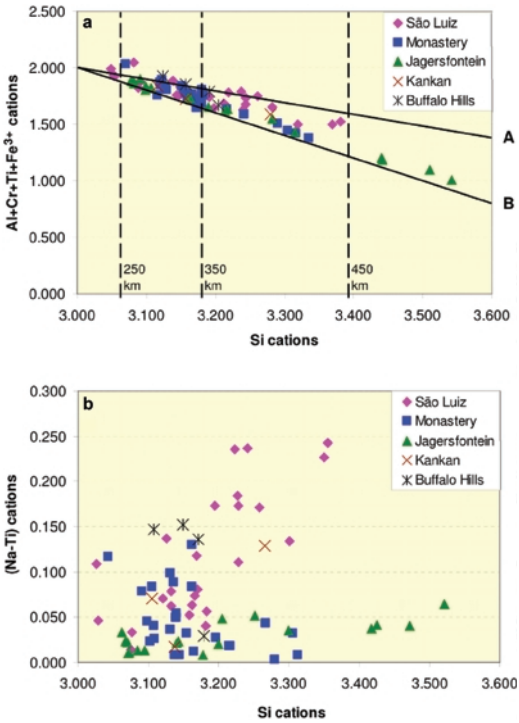

FIG. 4. Majoritic garnet inclusions of metabasite (= meta-eclogite) composition from the localities shown; for data sources see Table 3. (*a*) The sum of Al^{3+}+Cr^{3+}+Ti^{4+}+Fe^{3+} cations plotted against total Si atoms (on the basis of 12 oxygens p.f.u. with Fe^{3+} calculated according to the method of Droop, 1987). The increase of Si^{4+} (>3 cations) is associated with a decrease to <2 of Al^{3+}+Cr^{3+}+Ti^{4+}+Fe^{3+} cations (the typical *Y* site cations of a non-majoritic eclogitic garnet. The oblique lines indicate the trends of the two major combined substitutions: A represents the substitution where Si^{4+} on the *Y* site is charge-balanced by Na on the *X* site; B represents the substitution where Si^{4+} on the *Y* site is charge balanced by R^{2+} substitution on the *Y* site (see text). The depths indicated are based Si^{4+} cation compositions (for 12 oxygens p.f.u.) in the high *P-T* experiments of Akaogi and Akimoto (1979) and Irifune (1987). (*b*) ($Na^{+}-Ti^{4+}$) cations plotted against Si^{4+}, to illustrate the varying extent to which Si substitution in the *Y* site is charge-balanced by Na^{+} substitution. Ti^{4+} is subtracted from Si^{4+}, on the assumption that Na^{+} also charge-balances any Ti^{4+} present.

line A in Fig. 4*a*), whilst in the second case, two trivalent cations are lost for every Si^{4+} cation substituted (shown as trend line B in Fig. 4*a*). For the majoritic garnets found as inclusions in diamonds, it is evident from Fig. 4 that both of these substitution mechanisms operate, but to varying degrees at different localities. Such variations are emphasized in Fig. 4*b*, illustrating Na^{+} abundance (plotted as $Na^{+}-Ti^{4+}$) relative to Si^{4+} cation abundance. The Na^{+} abundance is plotted as ($Na^{+}-Ti^{4+}$) on the basis that Na^{+} may also be charge-balancing any Ti^{4+} present, and therefore any such Na^{+} cannot simultaneously charge-balance Si^{4+}. Figure 4*b* emphasizes the marked differences in Na^{+} abundance and the extent of the coupled NaSi substitution between the São Luiz and Jagersfontein localities. One might speculate that this difference affected the kinetics of exsolution during decompression, and that large Na contents promoted clinopyroxene exsolution in the case of São Luiz.

Broad pressure estimates for the formation of analysed majoritic garnets are given in Table 3 and plotted in Fig. 4. They are based on the experimental data from Akaogi and Akimoto (1979) and particularly Irifune (1987), and are based on the Si^{4+} cation content per formula unit of 12 oxygens in the experimental compositions. Unfortunately, the separate effects of the above two principal substitution mechanisms have not been experimentally evaluated, and it must therefore be emphasized that the pressure estimates given are very provisional. Other potential problems must be recognized for these estimates. Many of them are based upon EMPA point analyses and such analyses may be affected by variable amounts of clinopyroxene exsolution from an intial more Si-rich majorite composition. In the case of São Luiz, Harte and Cayzer (2007) used modal analysis to obtain estimates of original majorite (bulk) compositions prior to exsolution, and these bulk compositions provide the maximum estimate of Si^{4+} cations p.f.u. for São Luiz in Table 3.

One effect of clinopyroxene exsolution is that estimates of the depths of formation of majorite, based on single majorite analyses, rather than recombined garnet and clinopyroxene analyses, are going to be minima. Yet another factor that will result in depth estimates being lower than true initial depth of formation values, is the bulk composition of the majorites. Once a depth of complete solid solution of clinopyroxene in majorite is attained, then the majorite composition can remain fixed even if taken to higher pressures (Harte and Cayzer, 2007).

Taking the pressure estimates summarized in Table 3 and Fig. 4 at face value would indicate

that the great majority of majorite inclusions formed at ~8 to 14.5 GPa (~240–440 km depth), but the lower values may well be affected by clinopyroxene exsolution, and in the case of São Luiz, Harte and Cayzer (2007) suggest the probability that many inclusions originated in the depth region 400 to 450 km, i.e. near the upper boundary of the TZ. The Jagersfontein inclusions, being without clinopyroxene, escape the problem of clinopyroxene exsolution and as such probably provide the best maximum depth estimate of ~500 km (Tappert *et al.*, 2005*a*,*b*). Overall, it seems likely that most of the metabasite majoritic garnets originated in the depth range of 300 to 500 km.

In considering the origin of the majoritic inclusions with metabasic bulk compositions, other aspects of geochemistry provide definite information on conditions of formation and protoliths. The *REE* compositions of majorite inclusions show great diversity (Fig. 5), from extremely depleted in *LREE* to flatter MORB-like patterns, whilst others show prominent *HREE* variation. This diversity applies to individual localities (e.g. Monastery, São Luiz, Jagersfontein) as well as to the dataset as a whole. It is most likely that such wide variations in trace-element abundances involve variable amounts of both melt extraction and enrichment, and Stachel *et al.* (2000*a*) suggest the involvement of carbonatitic melts.

Inclusions of metaperidotite and metabasite affinity from the lowermost TZ, the UM/LM boundary region and uppermost LM

The inclusions within diamonds from these depths show much more diversity than those from the asthenosphere and upper TZ. At least seven chemically defined primary silicate minerals occur, including SiO_2. Ferropericlase is a commonly associated mineral indicating metaperidotite bulk compositions in many cases. Usually, the initial inclusions have been formed by a single phase, but they may now consist of several phases as a result of retrogression which commonly affects the mpv and cpv phases (e.g. Harte *et al.*, 1999*b*; Joswig *et al.*, 1999; Stachel *et al.*, 2000*a*) and the conversion of the perovskite phases to higher-volume phases with decompression causes internal deformation of the diamonds (Cayzer *et al.*, 2008). A single diamond may contain several

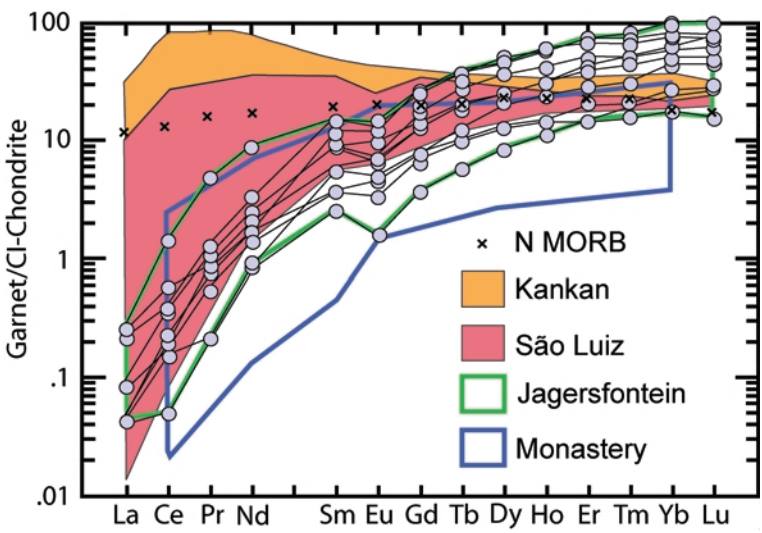

FIG. 5. Chondrite-normalized compositions of *REE* in majorites showing the wide spread of compositions from São Luiz, Jagersfontein and Monastery; and the lesser spread from Kankan. Only the overall range of compositions is given for São Luiz, Monastery and Kankan (which overlaps little with São Luiz). For Jagersfontein, individual sample compositions are also shown by the linked blue-grey dots. The average composition of N-MORB is shown for comparison. Based primarily on data from: Moore *et al.* (1991), Harte (1992), Stachel *et al.* (2000*a*) and Tappert *et al.* (2005*a*); and adapted from Tappert *et al.* (2005*a*).

inclusions of two or more separate phases and sometimes there are multiple inclusions in one diamond of the same phase. The occurrence of both multiple and composite inclusions is becoming more apparent as more sophisticated electron microscope, Raman spectroscopy and X-ray fluorescence techniques are employed (e.g. Brenker *et al*., 2002, 2005). Hayman *et al.* (2005) record many examples of multiple inclusions in diamonds from Rio Soriso, and in one extreme case a single diamond is reported with 21 inclusions belonging to five different phases (fPer, mpv, cpv, TAPP and Mg_2SiO_4).

At my last count, 251 diamonds have been reported with inclusions which might be derived from the lowermost UM and the uppermost LM. However, in 167 of these diamonds, the inclusions are just of a single phase, most commonly fPer, and it is not impossible that they have formed in special bulk compositions at shallower depths (e.g. Brey *et al.*, 2004). Sixty diamonds show inclusions of two or more phases and in 55 of these cases one or more silicates of probable ultrabasic and basic composition are involved. These silicate-bearing associations are the critical ones for comparison with the model ultrabasic and basic mineralogies of Fig. 2 and Table 2. In identifying the minerals of these associations, it must be noted that the silicates have commonly undergone retrogression to lower pressure phases, although their chemical compositions are believed to have been preserved by the encapsulating diamonds (e.g. Harte *et al.*, 1999*a*; Stachel *et al.*, 2000*b*). Thus, mpv inclusions which have co-existed with fPer are marked by small Ni concentrations by comparison with low-pressure orthopyroxene phases, and such features give confidence in the identification of deep mantle phases and associations (Stachel *et al.*, 2000*b*, 2005).

In Table 4, these associations are placed in three groups. The first group has associations which are placed in the UM/LM boundary zone (Table 2) because of the association of the Mg_2SiO_4 phase with fPer and mpv (i.e. the UM/LM boundary reaction phases). Some uncertainty exists in some of these cases where single composite inclusions contain several phases and it is possible that the Mg_2SiO_4 phase has formed by retrograde reaction of touching fPer + mpv upon decompression (Stachel *et al*., 2000*a*; Brey *et al*., 2004; Hayman *et al*., 2005). In such a situation, the inclusion would have originated in the LM (group 2a). In other cases the Mg_2SiO_4 + mpv + fPer phases occur as separate inclusions in a single diamond and therefore clearly indicate the UM/LM boundary zone assemblage.

Group 2 (a and b) in Table 4 is placed within the LM because of the occurrence of mpv and/or fPer without Mg_2SiO_4. The distinction between 2a and 2b is that the mpv in group 2b is Al-bearing and indicates greater depths in the upper LM, where Al comes to reside in mpv rather than a garnet phase (Fig. 2 and Table 3). The experimental data show that formation of Al-bearing mpv is to be expected at within ~100 km of the top of the LM (Fig. 2; see also Irifune *et al.*, 1996; Hirose *et al.*, 2001), and thus its presence within the inclusions does not necessarily imply an origin from great depths within the LM.

The associations listed in group 3, (Table 4), cannot be located in the depth zones (Fig. 2 and Table 2) very precisely, and might belong in any of the depth zones indicated by groups 1, 2a, 2b above, or in the lower TZ. The inclusions with 'Na-Al pyroxene' phases are believed to have originally been a majoritic garnet phase at depth, and, from experimental data, are placed close to the UM/LM boundary (Gasparik and Hutchison, 2000; Hutchison *et al.*, 2001). The experimental work on these assemblages also suggests that they co-existed with cpv and a carbonate melt. A possibly related inclusion is an Na-Px-En inclusion described by Wang and Sueno (1996).

Arguably, many of the associations in group 3 have actually crystallized under the same conditions as the inclusions in groups 1 and 2, but the diamonds did not enclose a full set of the minerals present at the time of diamond crystallization. From this viewpoint, it is possible that all the associations in Table 4 could come from the relatively narrow depth range of 600 to 800 km (cf. Table 2 and Fig. 2).

Protoliths and evidence of subducted rock compositions

The mantle is clearly a dynamic environment, affected by subduction, convection, and rising plumes (e.g. Bercovici, 2007), and it is important to consider the origin of the materials which form the inclusions, their host diamonds, and the fluids/melts from which they may have crystallized. Specific evidence for the initial origin of the ultrabasic and basic rock compositions giving rise to the inclusions is rather limited. However, both positive and negative Eu anomalies have been detected in cpv inclusions, and these suggest

TABLE 4. Mineral associations of ultrabasic and basic composition found in single diamonds assigned to the lower Transition Zone and Lower Mantle.

Mineral associations	No. of diamonds	Locations[1]	Diamond ($\delta^{13}C$‰)
(1) UM/LM boundary associations with Mg_2SiO_4 phase, fPer and mpv			
fPer + mpv[2] + Mg_2SiO_4[3]	2	Rio Soriso (1)	
		DO27 (1)	−5.3
fPer +mpv + cpv + Mg_2SiO_4	1	Kankan	−4.1
fPer + mpv + TAPP + Mg_2SiO_4	1	Rio Soriso	–
fPer + mpv + cpv + TAPP + Mg_2SiO_4	1	Rio Soriso	
(2a) LM associations in the low-Al mpv facies/depth zone			
fPer + mpv[2]	4	Orroroo (1)	−3.8
		São Luiz (2)	
		Koffiefontein (1)	−5.3
		Kankan (1)	−3.9
fPer + mpv + TAPP	2	São Luiz (1)	−5.0
		Kankan (1)	
fPer + mpv + cpv	2	Kankan (1)	−4.1
		DO27 (1)	
fPer + mpv + cpv + Si-Mg phase	1	DO27	
fPer + mpv + Ni	1	DO27	−4.3
mpv + TAPP	2	Juina (1),	−5.1
		São Luiz (1)	−4.7
(2b) LM associations in the hi-Al mpv facies/depth zone			
fPer + mpv(Al)[2]	1	São Luiz	−5.3
fPer + mpv(Al) + crn	1	São Luiz	−5.3
(3) Associations possibly from the lower Transition Zone and UM/LM boundary region			
fPer + 'NaAl-pyroxene'/grt[4]	1	São Luiz	−5.3
TAPP + 'NaAl-pyroxene'/grt[4]	1	São Luiz	
maj + 'NaAl-pyroxene'/grt[4]	1	São Luiz	−5.1
fPer + SiO_2[3]	10	São Luiz (1)	
		Kankan (1)	−4.4
		Juina (1)	
		DO18(2), Panda	−4.9
		Rio Soriso (4)	
fPer + TAPP	3	São Luiz	−4.9
fPer + TAPP + Mg_2SiO_4[3]	1	São Luiz	−5.3
fper + Mg_2SiO_4	4	Kankan (2)	−3.8 and −3.9
		Juina (1)	−5.0
		Panda(1)	
fPer + Mg_2SiO_4 + MgAl-spinel	1	Panda (1)	
fPer + cpv	8	São Luiz (3)	
		Rio Soriso (3)	
		Kankan (2)	−5.8, and −4.7
		Panda (1)	
cpv + Mg_2SiO_4		Juina (1)	−4.9
cpv + SiO_2	2	Kankan (1)	
		Juina(1)	
cpv + SiO_2 + FeS	1	Kankan	
cpv + Ni	1	Juina	−4.3

[1] References for the localities are as follows: São Luiz – Harte *et al*. (1999*b*); Hutchison (1997); Hutchison *et al*., (1999, 2001). Kankan – Stachel *et al*. (2000*b*, 2002). Juina – Kaminsky *et al*. (2001, 2009); Bulanova *et al*. (2010). Rio Soriso – Hayman *et al*. (2005). Koffiefontein – Moore *et al*. (1986); Deines *et al*. (1991). DO27 – Davies *et al*. (1999, 2004*a*). Panda – Tappert *et al*. (2005*c*). Orroroo – Tappert *et al*. (2009*a*,*b*).
[2] mpv refers to low-Al MgSi-perovskite, and mpv(Al) refers to high-Al MgSi-perovskite (see also Table 1).
[3] Mg_2SiO_4 and SiO_2 are used to refer to phases of those compositions as the original included polymorphs are usually uncertain.
[4] 'NaAl-pyroxene'/garnet refers to an NaAl-rich pyroxene phase that is thought to have formed as garnet (Hutchison *et al*., 2001).
A very small number of fPer-bearing diamonds with uncertain other inclusions has been omitted.

formation from protoliths derived from the plagioclase stability field in the crust, and therefore the presence of subducted material at the point of formation of the diamonds and their inclusions (Harte *et al*., 1999*b*; Stachel *et al*., 2000*b*, 2005). Evidence of negative Eu anomalies has also been found in some majoritic garnets, particularly those from Jagersfontein, and Tappert *et al.* (2005*a*,*b*) argue strongly for their origin from subducted and metamorphosed oceanic crust.

Very recently, detailed studies have directed attention to a minor group of inclusions indicating distinct highly calcic and sometimes Ti-rich bulk compositions. These have been found in diamonds from Kankan (Brenker *et al.*, 2005) and especially Juina (Brenker *et al.*, 2007; Walter *et al.*, 2008; Kaminsky *et al*., 2009; Bulanova *et al*., 2010). Inclusions of $CaSiO_3$, $CaTiO_3$, $CaSi_2O_5$, and calcic garnet/majorite are recorded, and the *P-T* conditions of formation appear to be in the lower asthenosphere and the TZ, at depths which largely overlap those of majorite inclusions discussed above. In addition, micro-inclusions of Ca-Mg-Fe carbonates have been found (Brenker *et al.*, 2007; Walter *et al.*, 2008; Bulanova *et al.*, 2010), and very rare inclusions of Al-rich silicates (Wirth *et al.*, 2007; Bulanova *et al.*, 2010). Clearly, they provide strong evidence for the involvement of subducted material derived from oceanic sedimentary sequences. The occurrence of such inclusions, at localities with prominent suites of 'deep' mantle basic and ultrabasic inclusions, lends further credibility to the wide involvement of subducted material.

Diamond characteristics

The diamonds containing 'deep' mantle inclusions show a distinctive combination of characteristics which are briefly summarized here for their bearing on carbon source compositions and mantle residence times. Commonly, the diamonds are dodecahedroid to irregular in morphology, indicating the occurrence of some resorption; and they have also commonly been affected by external plastic deformation (Hutchison, 1997; Hutchison *et al.*, 1999; Kaminsky *et al.*, 2001; Stachel *et al.*, 2002; Davies *et al.*, 1999, 2004*a*). Few cathodoluminescence (CL) studies on growth structures in deep mantle diamonds have been conducted because they show poor CL response. However, Hutchison (1997) and Hutchison *et al.* (1999) show the occurrence of concentric growth structures which suggest growth in a fluid/melt.

In terms of geochemical parameters, both the diamonds with majoritic inclusions and those from near the UM/LM boundary and LM are commonly found to be very poor in nitrogen (Hutchison, 1997; Hutchison *et al.*, 1999; Kaminsky *et al.*, 2001; Stachel *et al.*, 2002; Davies *et al.*, 1999, 2004*a*,*b*; Cartigny, 2005). Thus, they are commonly classified as Type II, meaning that their N content is too low to be detected by FTIR. The explanation of this very marked geochemical feature is uncertain. Ion microprobe studies of diamonds show variations from <100 ppm to >1000 ppm in very narrow growth zones in lithospheric diamonds (e.g. Harte *et al.*, 1999*a*). Likewise, ion microprobe studies on LM diamonds show that substantial small-scale variations can occur within single diamonds; Hutchison *et al.* (1999) record a variation from 0.1 to 260 ppm. It is therefore unclear to what extent N content is controlled by growth kinetics rather than bulk geochemical reservoir composition (e.g. Hutchison *et al.*, 1999; Cartigny *et al.*, 2001).

The aggregation state of N in diamonds has been shown to be dependent on the abundance of N, and their temperatures and times of residence in the mantle (Evans, 1992). The aggregation state of N has been determined on both majoritic and UM/LM boundary and LM diamonds, and in most cases a very high proportion (typically >>50%) of N is in the more-aggregated B state, rather than in the less-aggregated A state This is a high ratio compared with lithospheric diamonds, and suggests storage in the mantle at high temperatures or over long periods of time, or both (Hutchison, 1997; Hutchison *et al.*, 1999; Tappert *et al.*, 2005*a*, 2009*a*). Clearly these features might be expected for diamonds formed in the sublithospheric mantle, and potentially residing there for tens of millions of years. However, a small number of exceptions exist, with A-state N aggregation being dominant and implying relatively short mantle residence times (e.g. Stachel *et al.*, 2002; Tappert *et al.*, 2005*a*). Such exceptions are most often seen amongst diamonds bearing asthenosphere and upper TZ inclusions, rather than those with UM/LM boundary and LM inclusions.

The prime geochemical information gathered on all natural diamonds is their C isotope composition (Cartigny, 2005). In this parameter, there are marked distinctions between the diamonds bearing majoritic garnets and those from around the UM/LM boundary and LM. The

diamonds of deeper origin, with dominantly metaperidotitic inclusions, have 'normal' mantle $\delta^{13}C$ values, largely in the range −3 to −6‰, with a concentration at −4 to −5‰ (see Table 4 for data on specific inclusion associations, and Cartigny (2005), for comparison with other worldwide data). Such values are typical values for mantle C from several sources. On the other hand, majorite-bearing diamonds of metabasic affinity show marked departures from the expected mantle norm. With the prominent exception of those from Kankan, diamonds with majoritic garnet inclusions have light C with negative $\delta^{13}C$ values largely in the range −10 to −24‰ (see Table 3). The particularly high negative values are potentially indicative of derivation from living tissues and have been the subject of much debate concerning identification of original crustal material in the mantle (e.g. Kirkley *et al.*, 1991; Cartigny *et al.*, 2001). For the exceptionally highly negative values from Jagersfontein of −17 to −24‰ (Table 3), a derivation from crustal material is supported by the Eu anomalies referred to above, and Tappert *et al.* (2005*a*,*b*) suggest these $\delta^{13}C$ values may derive from microbes in altered ocean-floor basalts (Torsvik *et al.*, 1998). Other evidence supporting a crustal origin for highly negative $\delta^{13}C$ values has come from oxygen isotope studies (Schulze *et al.*, 2003), and in some cases there is evidence of diamonds showing a transition from highly negative (crustal?) values towards more normal mantle values (Schulze *et al.*, 2004; Bulanova *et al.*, 2010). Such transitional $\delta^{13}C$ compositions could include those of the only moderately negative majorite-bearing diamonds and may imply a mixing of crustal and mantle sources in the formation of these diamonds. The unusual inclusions described by Bulanova *et al.* (2010) show a similar range of $\delta^{13}C$ values to the majorite-bearing inclusions.

As noted above, the Kankan diamonds carrying majoritic inclusions are exceptions to the general occurrence of light C isotope compositions in majorite-bearing diamonds, and show values from 0.9 to −3.1 $\delta^{13}C$‰ (Table 3; and Stachel *et al.*, 2002). Stachel *et al.* (2005) point out that the near zero $\delta^{13}C$ values correspond with those of carbonate sediments. Some evidence of a mixing trend towards carbonate $\delta^{13}C$ values is also noted for the Eurelia (Orroroo) diamonds (Tappert *et al.*, 2009*a*). Considering the evidence for subducted protoliths at geographic locations ranging from São Luiz/Juina (Brazil) through Jagersfontein (South Africa) to Eurelia (south Australia), Tappert *et al.* (2009*a*) suggest the sublithospheric diamonds at all these localities derived from remnants of the subducted proto-Pacific plate at the margin of Gondwana.

Discussion

Diamonds from two principal depth zones

The minerals and mineral associations described above provide clear evidence for the occurrence of diamonds bearing inclusions from the asthenosphere, TZ and LM (Table 2). With the exception of the occurrence of TAPP, rather than garnet, in diamonds from the UM/LM boundary region, the mineral associations of the inclusions match those predicted from experimental data (Table 2). Although the numbers of diamonds containing such inclusions is small they have been found worldwide (Tables 3 and 4) and consistently point to formation in the two main depth regions:

(1) in the lower asthenosphere and upper TZ (possibly 300−500 km) with dominantly metabasite inclusions;

(2) around the region of the UM/LM boundary and into the LM (possibly 600−800 km) with dominantly metaperidotite inclusions. The marked dominance of basic inclusions in one depth zone and ultrabasic ones in the other must also be emphasized.

These features of distribution are not believed to imply worldwide depth zones of particular compositions (Stachel, 2001; Stachel *et al.*, 2005), and clearly require explanation. Even within the 600 to 800 km depth region, the distribution shows special features. The associations in group 1 of Table 4 where olivine inclusions are separate from fPer and mpv in the same diamond clearly point to formation at the conditions of the UM/LM boundary reaction. This boundary, from experimental data, is expected to be quite sharp, with a very narrow depth interval (Ito and Takahashi, 1989; Fei *et al.*, 1991, 1996), and the occurrence of the boundary minerals as an association of inclusions in single diamonds suggests the possibility that this depth zone is a focus for diamond formation.

In seeking a cause for such preferential depth and compositional distribution of diamonds and inclusions, the general evidence noted in the introduction, that natural diamonds characteristically form in fluids/melts, must be considered. In addition, we have noted specific features, such as the variable *REE* compositions of majoritic

inclusions (Fig. 5), as providing evidence for the involvement of melts in inclusion formation. Below the asthenosphere, melting of dry ultrabasic and basic rocks lacking C-O-H volatiles is unlikely. In considering locations for volatiles and especially H_2O in the mantle, and the associated potential for melt formation, much attention has been paid to the TZ because the two key solid phases, wadsleyite and ringwoodite have been shown capable of holding up to 3 wt.% H_2O (e.g. Smyth, 1987; Inoue *et al.*, 1995; Ohtani, 2005; Kawamoto, 2006). Whether or not these phases actually contain significant H_2O in the real UM is very hard to say (see especially discussion in Karato, 2006). If H_2O is present, obvious questions arise concerning the derivation of the H_2O, and whether significant H_2O transport from the lithosphere and hydrosphere is possible. In order to consider the possibilities for H_2O transport, fluid generation and melting in the deep mantle, we must examine the great downward transport system of oceanic lithosphere in subduction zones. Particular interest is also directed to this subject because of the evidence discussed above for the involvement of subducted protoliths in deep diamond inclusions.

Dehydration of subducting oceanic lithosphere and diamond formation in the region of the lowermost TZ and upper LM

The metamorphism of subducting oceanic lithosphere as it descends into the UM has been investigated widely, and the stability of hydrous phases at relevant pressure-temperature conditions documented. Penetration of ocean water into the ocean lithosphere to create hydrous bulk compositions occurs at ocean ridges, but is probably of most significance as a result of bending and cracking of the plate just prior to subduction (Grevemeyer *et al.*, 2007). From the viewpoint of deeper subduction (below the levels of stability of formation of common lithospheric phases such as common amphiboles, epidote minerals and chlorites), we have to consider the stability relations of hydrous phases below ~3 to 4 GPa (90–120 km depth). These matters have been the subject of several recent reviews (Ohtani, 2005; Frost, 2006; Kawamoto, 2006; Karato, 2006; Komabayashi and Omori, 2006; Komabayashi, 2006). Kawamoto (2006) emphasizes that below these depths, the miscibility gap between aqueous fluids and peridotite melts disappears, whilst simultaneously the silicate components dissolved in H_2O-rich fluids start to acquire relative proportions of chemical constituents similar to peridotite itself. Also, at these depths, there is miscibility between siliceous and carbonatitic melts (Litvin *et al.*, 2008).

With these constraints in mind, much then depends on the temperatures within the slab and the stability relations of particular minerals. Within the metabasites of the original crustal portion of the slab, assuming low K_2O bulk compositions, the hydrous mineral most likely surviving to the greatest pressure/depth is lawsonite with an estimated maximum of depth of ~300 km (Kawamoto, 2006; Komabayashi, 2006).

The possibility of H_2O transport to greater depths lies in the metaperidotitic body of the slab, and depends on the stability relations of serpentine (antigorite) and a series of DHMS (denoted by alphabetical names: A, B, etc., e.g. Ohtani, 2005; Kawamoto, 2006; Komabayashi, 2006). In a recently derived petrogenetic grid for the reaction relations in model peridotite compositions, Komabayashi *et al.* (2004), Komabayashi and Omori (2006) and Komabayashi (2006) recognize four principal situations depending on the temperature within the subducting slab:

(a) *In a hot slab and the mantle wedge*: all water will be lost by dehydration at pressures <5.1 GPa and escape upwards; dry metaperidotite descends into the mantle.

(b) *In an initially cool slab, descending to the LM unaffected by stagnation and heating, two stages of dehydration are recognized.*

In the first stage (b_1), at pressures between 5 and 8.5 GPa, antigorite is replaced by dense hydrous phase A (plus orthopyroxene). The actual pressure of the transition is affected by bulk composition and aluminous compositions will form the intermediate phase Mg-sursassite (Bromiley and Pawley, 2002). The cool geotherms involved have to have temperatures below ~550ºC for Al-poor compositions, and below ~650ºC for Al-rich compositions. In a model hydrous peridotite bulk composition the breakdown of antigorite (nominally 12.3 wt.% H_2O) results in a decrease to 3.66 wt.% H_2O in solid phases (Fig. 6 and Komabayashi and Omori, 2006).

In the second stage (b_2), water loss occurs in the depth region of 27 to 30 GPa, with the breakdown of hydrous phase D and super-hydrous phase B (reactions 8 and 9 in Fig. 6). Thus, from the formation of dense hydrous phase A at 5 to 8.5 GPa up to pressures of ~27 GPa the water

content of the metaperidotite remains constant even though there is progressive formation of several DHMS (within the blue zone of Fig. 6). Beyond 30 GPa, hydrous solid phases are absent and with the escape of the hydrous fluid phase the metaperidotite becomes water free.

(c) *In an initially cool slab, which warms up and stagnates, water release from the solid phases will occur in two main depth zones, but will involve several sets of dehydration reactions in the lower zone.*

The first stage (c_1) is the same as that for case (b_1) above.

In the deep mantle stage (c_2), a series of dehydration reactions occur if the temperature rises above ~1200ºC within the TZ of the mantle. Initially, hydrous DHMS phases E and B will give rise to hydrous wadsleyite or hydrous ringwoodite, according to pressure (depth). Given that warming becomes more likely with increasing depth, so this stage of water release becomes more likely in the ringwoodite stability field in the lower part of the TZ. After hydrous ringwoodite formation, progressive subduction will then cause its breakdown with the formation of the characteristic mpv+fPer assemblage of the LM. The possible reactions (shown as reactions 4 to 7 in Fig. 6) depend on the precise *P-T* path resulting from stagnation and warming, as illustrated in Fig. 6. They occur in the 20 to 26 GPa depth region, and include the UM/LM boundary reaction.

(d) *In a very cold slab*: water passes into the DHMS phases eventually coming to reside in dense hydrous phase D which, for the temperatures concerned, remains stable to considerable depths in the LM.

The dehydration points noted above are summarized pictorially in the mantle cross-section of Fig. 7, where dehydration reaction positions 4, 5, 6 and 7 apply to case (c), and the deeper dehydration reaction positions of 8 and 9 apply to case (b). Both cases involve a set of shallow-level dehydration reactions (indicated by 1, 2 and 3 in Fig. 7), as well as the deep ones near the UM/LM boundary, and this bimodal depth distribution receives support from earthquake distributions in some subduction zones (Komabayashi *et al.*, 2004). In Fig. 7, the lower end of subducted slab is illustrated with several alternative situations in mind. Where penetration of a cold slab into the LM occurs, the likely result is the dehydration reaction positions shown by locations 8 and 9. Where stagnation and warming of the slab occur, then the locations for reactions 4 to 7 apply; in this case, Fig. 7 indicates schematically both the piling up of material at the UM/LM boundary (as in a megalith – Irifune

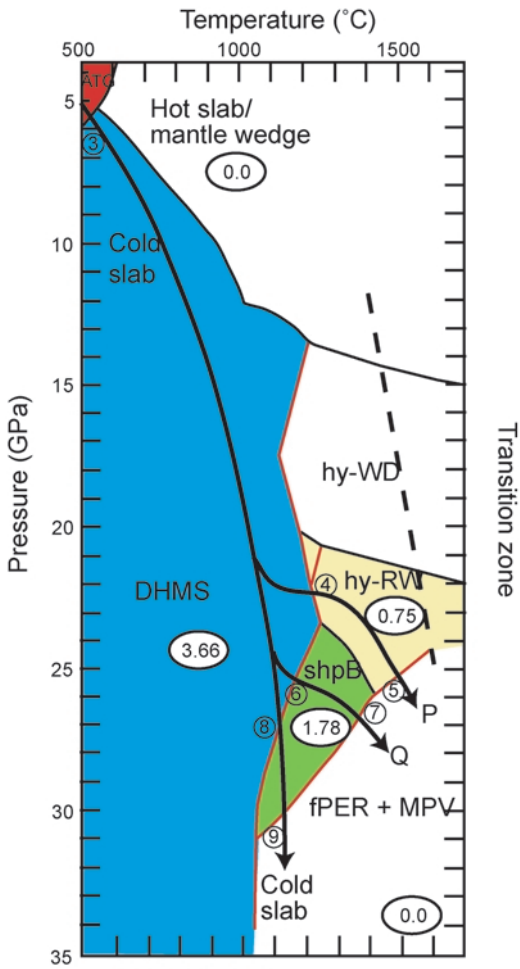

FIG. 6. Simplified *P-T* plot of phase relations for hydrous peridotite, adapted from Komabayashi and Omori (2006). The stability fields are shown for: atg, in red; DHMS, in blue; hy-wd, not coloured; hy-rw, in yellow; shpB, in green; and fPer + mpv, (not coloured). The dark lines show potential geotherms for a cold slab, with possible variations (P and Q) due to stalling and warming of the subducting slab. The dashed line indicates a normal average mantle geotherm. The red boundary lines denote dehydration reactions, with the numbers (3 to 9) identifying reactions also shown and itemized on Fig. 7. The numbers in oval boxes give wt.% H_2O for the fields concerned.

and Ringwood, 1987; Ringwood, 1991) and the possibility of deflection along the base of the TZ at the UM/LM boundary.

The release of H_2O in the dehydration reactions occurring in the lower part of the TZ and upper part of the LM will give rise to miscible fluids/melts with silicate and possibly carbonatitic components. These fluids/melts form potential loci for diamond formation, and thereby potential loci for formation of the set of diamond inclusions we have identified as forming in this depth range. It is particularly notable that one of the dehydration reactions involved is that of hydrous ringwoodite at the UM/LM boundary, thereby forming a direct link with the group (1) inclusions of Table 4, from the UM/LM boundary.

Dehydration zones and the formation of lower asthenosphere and upper TZ inclusions

We have noted that on the basis of Eu anomalies in majoritic garnets and the $\delta^{13}C$ values of their host diamonds, that the metabasite associations of the lower asthenosphere and upper TZ appear to have been formed from subducted material. Tappert *et al.* (2005*a*,*b*) suggest that the formation of the diamonds and inclusions occurs during subduction, whilst the material forms part of the

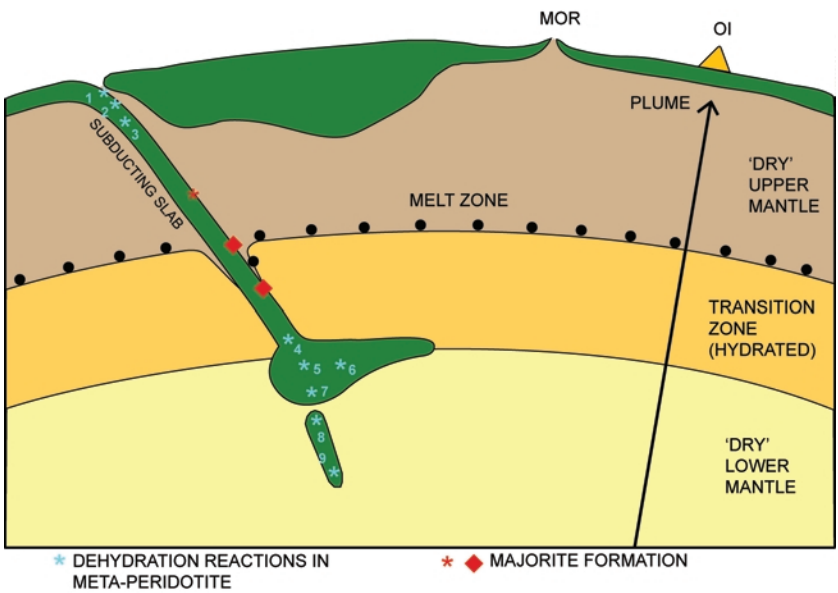

FIG. 7. Schematic Earth cross-section showing lithosphere (green), asthenosphere ('dry' Upper Mantle), Transition Zone, and upper part of the Lower Mantle. The sketch encompasses various possibilities for the lower end of the subducting slab including: penetration into the Lower Mantle; stalling with megalith formation; and bending along the base of the Transition Zone (e.g. King, 2007, see text). In the subducting slab, asterisks give the positions of key dehydration reactions after Komabayashi (2006), and Kawamoto (2006) as follows: **1** and **2** – various breakdown reactions of common crustal phases (talc, chlorites, Ca-Na amphiboles, epidotes); **3** – atg = hpA + en + fl; **4** – shpB + ak = hy-rw, and shpB + stv = ak + fl (warming slab; **5** – hy-rw = mpv + fPer + fl (warming slab; **6** – hpD + shpB = mpv + fl (warming slab); 7 – shpB = mpv + fPer + fl (warming slab); **8** – hpD + shpB = mpv + fl (cold slab); **9** – shpB = mpv + fPer + fl (cold slab). Reactions **3** to **9** take place in slabs with initially cool geotherms, but with some stagnation and heating taking place to give reactions **4** to **7** rather than **8** and **9** (see Fig. 6). Reactions **4** to **9** in metaperidotitic rocks may give rise to fluid/melt where diamonds crystallize with inclusions from the lower Transition Zone, Upper Mantle/Lower Mantle boundary and uppermost Lower Mantle. Potential locations of dehydration giving rise to the majoritic suite of diamonds (~300–500 km depth) are shown by the red star and red diamonds. The red star indicates the expected position of dehydration as a result of breakdown of lawsonite in subducted metabasites. The zone of dots is the potential locus of melts resulting from the dehydration of hydrous wadsleyite (after Bercovici and Karato, 2003), and the red diamonds indicate where such dehydration intersects the upper surface of the slab and might provide a locus for diamond formation with majoritic garnet inclusions.

crustally-derived upper portion of the subducting slab. The association of such diamond formation with dehydration reactions is not so clear cut as in the case of the deeper ultrabasic inclusions, but several possibilities exist.

Accepting the depth range of formation of ~300 to 500 km for these inclusions, there is one prominent dehydration reaction which may play an important role in metabasites and this is the breakdown of lawsonite at ~300 km (Kawamoto, 2006; Komabayashi, 2006) as shown on Fig. 7. Specific evidence of diamond and inclusion formation in this depth region is given by some of the unusual Ca-rich inclusions. Brenker *et al.* (2005) report the occurrence of a composite inclusion of Ca_2SiO_5 (with a titanite structure), β-Ca_2SiO_4 (larnite) and $CaSiO_3$ (retrogressive wahlstromite), in which the initial assemblage of Ca_2SiO_5 and Ca_2SiO_4 demands pressures of formation of 10 to 12 GPa. Thus, one may envisage the diamond carrying this inclusion to have formed in a Ca-rich crustal protolith as a consequence of fluid/melt formation caused by the dehydration of lawsonite in adjacent subducted crustal metabasites. Bulanova *et al.* (2010) also note the occurrence of a kyanite-bearing diamond which may also come from ~300 km depth.

As lawsonite is the phase in metabasites carrying structural H_2O to the greatest depths, there are no further dehydration reactions in metabasites which could be responsible for formation of diamonds with majorite inclusions in the deepest asthenosphere and TZ. However, the upper (crustal) surface of the subducting slab is expected to be in contact with metaperidotites of the adjacent mantle, which at the top of the TZ is marked by the olivine-to-wadsleyite transition. This transformation has been highlighted by Bercovici and Karato (2003), who note that if hydrous wadsleyite is present in the TZ, then its conversion to olivine will lead to the liberation of H_2O; this in turn will lead to the formation of a melt zone or at least pools of melt along the upper margin of the TZ. The position of this potential melt zone, adapted from Bercovici and Karato (2003) is shown by a series of dots in Fig. 7. These authors linked the formation of such a melt zone with processes controlling the formation of MORB and OIB, and considerable doubt about these aspects of their model has been expressed by Hirschmann *et al.* (2005). However, this does not refute the possibility of a potential zone of melting as a result of the hydrous wadsleyite-to-olivine transformation, and the locus of this zone of potential melts is marked by dots in Fig. 7 (following Bercovici and Karato, 2003). The intersection of this potential melt zone with the upper surface of the subducting slab, marked by red diamonds in Fig. 7, provides locations where melts are in contact with subducted metabasites, and therefore locations for the formation of diamonds and inclusions carrying evidence of crustal protoliths. In broad terms, we may note that the occurrence of hydrous wadsleyite and hydrous ringwoodite in the TZ is supported by the potential transport of DHMS minerals in the body of subducting slabs, as described in the preceding section (see also Komabayashi *et al.*, 2004; Komabayashi, 2006).

Recently, Bulanova *et al.* (2010) have considered the origin of Ca- and Ti-rich inclusion associations from Juina that appear to have formed over similar depths to the majoritic garnet metabasite inclusions. They suggest formation of diamonds and inclusions in a rising plume which intersects previously subducted material away from the actual subduction zone, and a plume model is preferred because they have a $^{206}Pb/^{238}U$ age on a Ca-Ti-Si perovskite inclusion allowing only ~8 Ma between diamond formation and kimberlite eruption. Bulanova *et al.* (2010) also suggest that heating gives rise to carbonatitic melts within which the inclusions and diamonds form. However, it appears possible that upwelling mantle carrying hydrous wadsleyite may again contribute to melt formation by water release on conversion to olivine.

From the viewpoint of the combined ultrabasic and basic suites of sublithospheric diamonds discussed in this paper, the Bulanova *et al.* (2010) model does not provide an explanation for the consistent depth distributions of the inclusions. Thus the model of formation in a plume intersecting and entraining previously subducted material does not explain the absence of metaperidotite associations from the lower asthenosphere and TZ. In the model advocated here, the restriction of metaperidotite associations to the UM/LM boundary and LM is determined by the depths of dehydration of DHMS in an initially cool subducting slab.

Diamond carbon isotope compositions in relation to dehydration zone models

We have noted previously that the $\delta^{13}C$ values of sublithospheric diamonds show some very definite features. The metaperidotite (UM/LM boundary and LM) inclusions have a clear,

dominant record of normal mantle (−3 to −6‰) compositions. On the other hand, basic and other inclusions from the asthenosphere and upper TZ commonly show $\delta^{13}C$ compositions from −10 to −24‰, in which the highest values potentially represent organic matter in sediments or altered basalts, and the lower values may represent mixing trends towards normal mantle compositions. In addition, some majorite-bearing diamonds show another trend in $\delta^{13}C$ to possible marine carbonate compositions of 0.9 to −3.1‰.

In both these cases, the $\delta^{13}C$ values of diamonds with majoritic inclusions show evidence of involvement of crustal material, which complements other evidence of the involvement of crustal protoliths. For the inclusions of ultrabasic nature, we have also noted some evidence of crustal protoliths in the form of occasional Eu anomalies, suggesting plagioclase-bearing protoliths, but the host diamonds show normal mantle $\delta^{13}C$ signatures near −5‰. I suggest that these values for the metaperidotite associations are essentially a direct result of their subducted oceanic lithosphere protoliths being of mantle origin in the first place. Hydration of the lithospheric peridotite is necessary in order for hydrous metaperidotite to be subducted and DHMS minerals to form. But, it is suggested that this hydration will occur at depths in the ocean lithosphere away from the influence of sediments and organisms such as thermophile bacteria that are implicated in the carbon isotope signatures of the metabasites derived from oceanic crust.

Conclusions

Comparison of the inclusions and associations of inclusions found in natural diamonds with experimentally-determined silicate assemblages to depths of ~800 km, shows a close correspondence between the natural and the experimental data. Thus, a series of depth zones or facies (Table 2) may be erected from the mineral assemblage data into which both the natural and experimental data fit. There is one significant departure in the natural occurrences from the experimental data, and that is in the occurrence of the mineral TAPP in assemblages from near the UM/LM boundary and in the uppermost LM in place of pyrope-rich and majoritic garnet.

Two major suites of inclusions of sublithospheric origin have been recognized in diamonds from worldwide locations. They are:

(1) A suite of majoritic garnet (±clinopyroxene) inclusions of basic composition from the asthenosphere and upper TZ (summary in Table 3).

(2) A suite of dominantly ultrabasic inclusions derived from the UM/LM boundary region and the uppermost part of the LM, showing associations involving mpv, fPer and cpv (summary in Table 4).

Although there are some uncertainties in precise depth estimates, it is suggested that the basic (metabasite) suite of inclusions comes from depths of 300 to 500 km, and the ultrabasic (metaperidotite) suite from depths of 600 to 800 km.

Inclusions of both suites show evidence of derivation from crustal protoliths by the presence of Eu anomalies in the *REE* patterns of majoritic garnet and cpv phases. Further evidence of subduction of crustal sources is seen in the rare occurrence of carbonates and Al-rich inclusions, implying sedimentary rock protoliths.

Given that natural diamonds are commonly thought to grow in fluids/melts, and that melting in the deep mantle is likely to be strongly controlled by the presence of volatile species, consideration has been given as to whether the abundance of inclusions from the above restricted depth zones may be linked to the occurrence of fluids/melts at these particular depths. Strong support for this hypothesis has been found from consideration of the distribution of hydrous minerals in the sublithospheric mantle and the loci where dehydration reactions may take place in subducting slabs to release H_2O, which may then cause melting. These results may be summarized as follows:

(1) In subduction zones with relatively cool geotherms, H_2O may be carried in DHMS within the metaperidotite part of the slab, which may undergo a variety of dehydration reactions: at lower TZ depths, along the UM/LM boundary, with the breakdown of hydrous ringwoodite, and also in the uppermost LM (Komabayashi, 2006). The precise reactions occurring will depend on the initial slab geotherm, the rate of subduction and whether the subducting slab undergoes stagnation and warming at depth – perhaps with the formation a of a megalith (summarized in Figs 6 and 7). The set of potential dehydration reactions in the depth range 600–800 km provides the potential basis for fluid/melt formation and diamond crystallization with mineral inclusion capture.

(2) In metabasite assemblages, lawsonite is expected to be the hydrous phase stable to the greatest depths, and with an upper pressure

stability limit of ~10 GPa, this could provide a mechanism for fluid release and melt formation at ~300 km, which is appropriate for the shallower majorite suite inclusions.

(3) The Mg_2SiO_4 phases, wadsleyite and ringwoodite, from the TZ, are potentially hydrous and may thus store H_2O in the TZ. A mechanism for transport of H_2O down to the TZ and formation of hydrous Mg_2SiO_4 silicates is provided by the processes of (1) above.

(4) A fluid/melt zone potentially exists at the top of the TZ where hydrous wadsleyite breaks down to less hydrous olivine in upwelling mantle (Bercovici and Karato, 2003). Because the majoritic inclusions are exclusively metabasic rather than metaperidotitic in composition, an ideal locus for the formation of these inclusions will occur where a fluid/melt zone formed by breakdown of hydrous wadsleyite intersects the upper surface of metamorphosed ocean floor basalts on a subducting slab. This provides a possible mechanism for the formation of the deeper majorite suite inclusions.

The interpretations outlined above associate the formation of basic and ultrabasic deep mantle inclusions and their diamonds with subduction zones, and dehydration reactions occurring in subducted material or at the subduction interface. The restricted *P-T* conditions of dehydration reactions for appropriate minerals provide the constraints for limiting depths of melt formation and locations for diamond growth. Simultaneously, the locations of the reactions determine which rock bulk compositions may be affected and contribute to inclusions.

The hypotheses suggested are also in harmony with the $\delta^{13}C$ compositions of the host diamonds. The formation of the asthenosphere and upper TZ suite diamonds from fluid interaction with crustal protoliths in the subducting slab will explain the evidence of both organic and sedimentary sources in the $\delta^{13}C$ signatures of the majorite suite diamonds. In addition, the spread of $\delta^{13}C$ values in majorite-bearing diamonds, from −24‰ towards normal mantle values, may be explained by interaction at the interface of subducted crust and host mantle. In contrast, the normal mantle $\delta^{13}C$ compositions near −5‰ in the UM/LM and LM inclusions may simply reflect the recycling of mantle peridotite signatures through the oceanic lithosphere and back to the deep mantle without contamination by crustal sources.

Once formed, the inclusions will be protected from outside geochemical influence by the encapsulating diamond and may reside at depth for some time. Eventually, upward convection or plumes must start the material on its journey to the Earth's surface. It is a case for further speculation whether this journey might be in a single stage, or involve a period of residence in the lower lithosphere (e.g. Griffin *et al.*, 1999; Harte and Cayzer, 2007) from whence the deep diamonds are transported to the surface together with mantle xenoliths and other diamonds from the mantle lithosphere.

Acknowledgements

Many people have contributed to my interests in the subject of this paper, and I would particularly wish to thank Jeff Harris and John Gurney for past collaborations. The research scientists of the Edinburgh Materials and Micro-Analysis Centre (EMMAC) are also thanked for help and encouragement in pursuing relevant analytical studies. Richard Taylor and Jenny Rapp have been very helpful in drafting diagrams. Felix Kaminsky, Maya Kopylova and Thomas Stachel helped considerably by providing spreadsheets and detailed descriptions for analytical data from prime localities. Pierre Cartigny, Ed Grew, Graham Pearson and Thomas Stachel are thanked for conscientious and thought-provoking reviews. This paper is based upon the presentation of the 2009 Hallimond Lecture, and I thank the Mineralogical Society of Great Britain and Ireland for the invitation to give this lecture.

References

Akaogi, M. and Akimoto, S. (1979) High pressure phase equilibria in a garnet lherzolite, with special reference to Mg^{2+}-Fe^{2+} partitioning among constituent minerals. *Physics of the Earth and Planetary Interiors*, **19**, 31–51.

Bercovici, D. (editor). (2007) Mantle Dynamics. Vol. 7 in: *Treatise on Geophysics*, editor-in-chief, G. Schubert, Elsevier, Amsterdam.

Bercovici D. and Karato, S-I. (2003) Whole-mantle convection and the transition-zone water filter. *Nature*, **425**, 39–44.

Brenker, F.E., Stachel, T. and Harris, J.W. (2002) Exhumation of lower mantle inclusions in diamond: a TEM investigation of retrograde phase transitions, reactions and exsolution. *Earth and Planetary Science Letters*, **198**, 1–9.

Brenker, F.E., Vincze, C., Vekemans, B., Nasdala, L., Stachel, T., Vollmer, C., Kersten, M., Somogyi, A.,

Adams, F., Joswig, W. and Harris, J.W. (2005) Detection of a Ca-rich lithology in the Earth's deep (>300 km) convecting mantle. *Earth and Planetary Science Letters*, **236**, 579–587.

Brenker, F.E., Vollmer, C., Vincze, C., Vekemans, B., Szmanski, A., Janssens, K., Szaloki, I., Nasdala, L., Joswig, W. and Kaminsky, F. (2007) Carbonates from the lower part of the transition zone or even the lower mantle. *Earth and Planetary Science Letters*, **260**, 1–9.

Brey, G.P., Bulatov, V., Girnis, A., Harris, J.W. and Stachel, T. (2004) Ferropericlase – a lower mantle phase in the upper mantle. *Lithos*, **77**, 655–663.

Bromiley, G.D. and Pawley, A.R. (2002) The high-pressure stability of Mg-sursassite in a model hydrous peridotite: a possible mechanism for the deep subduction of significant volumes of H_2O. *Contributions to Mineralogy and Petrology*, **142**, 714–723.

Bulanova, G.P., Walter, M.J., Smith, C.B., Kohn, S.C., Armstrong, L.S., Blundy, J. and Gobbo, L. (2010) Mineral inclusions in sublithospheric diamonds from Collier 4 kimberlite pipe, Juina, Brazil: subducted protoliths, carbonated melts and primary kimberlite magmatism. *Contributions to Mineralogy and Petrology*, DOI 10.1007/s00410-019-0490-6.

Cartigny, P. (2005) Stable isotopes and the origin of diamond. *Elements*, **1**, 79–84.

Cartigny, P., Harris, J.W. and Javoy, M. (2001) Diamond genesis, mantle fractionations and mantle nitrogen content: a study of δ13C-N concentrations in diamonds. *Earth and Planetary Science Letters*, **185**, 85–98.

Cayzer, N.J., Odake, S., Harte, B. and Kagi, H. (2008) Plastic deformation of lower mantle diamonds by inclusion phase transformations. *European Journal of Mineralogy*, **20**, 333–339.

Davies, R.M., Griffin, W.L., Pearson, N.J., Andrew, A.S., Doyle, B.J. and O'Reilly, S.Y. (1999) Diamonds from the deep: pipe DO-27, Slave craton, Canada. Pp. 148–155 in: *Proceedings of the VIIth International kimberlite Conference, J.B. Dawson volume*, (J.J. Gurney, J.L. Gurney, M.D. Pascoe and S.H. Richardson, editors). Red Roof Design, CapeTown, RSA.

Davies, R.M., Griffin, W.L., O'Reilly, S.Y. and Doyle, B.J. (2004*a*) Mineral inclusions and geochemical characteristics of microdiamonds from the DO27, A154, A21, A418, DO18, DD17 and Ranch Lake kimberlites at Lac de Gras, Slave craton, Canada. *Lithos*, **77**, 39–55.

Davies, R.M., Griffin, W.L., O'Reilly, S.Y. and McCandless, T.E. (2004*b*) Inclusions in diamonds from the K14 and K10 kimberlites, Buffalo Hills, Alberta, Canada: diamond growth in a plume? *Lithos*, **77**, 99–111.

Dawson, J.B. (1989) Geographic and time distribution of kimberlites and lamproites: relationships to tectonic processes. Pp. 323–342 in: *Kimberlites and Related rocks, Vol.1: Their Composition*, *Occurrence*, *Origin and Emplacement.* Geological Society of Australia, Special publication No **14**.

Deines, P. (1980) The carbon isotopic composition of diamonds: relationship to diamond shape, color, occurrence and vapor compositon. *Geochimica et Cosmochimica Acta*, **44**, 943–961.

Deines, P., Harris, J.W. and Gurney, J.J. (1991) The carbon isotope composition and nitrogen content of lithospheric and asthenospheric diamonds from the Jagersfontein and Koffiefontein kimberlites, South Africa. *Geochimica et Cosmochimica Acta* **55**, 2615–2625.

Droop, G.T.R. (1987) A general equation for estimating Fe^{3+} concentrations in ferromagnesian silicates and oxides from microprobe analyses, using stoichiometric criteria. *Mineralogical Magazine*, **51**, 431–435.

Eskola, P. (1920) The mineral facies of rocks. *Norsk Geologisk Tidskrift*, **6**, 143–194.

Evans, T. (1992) Aggregation of nitrogen in diamond. Pp. 259–290 in: *The properties of natural and synthetic diamond* (J.E. Field, editor). Academic Press, London.

Fei, Y. and Bertka, C.M. (1999) Phase transitions in the Earth's mantle and mantle mineralogy. Pp.189–207 in: *Mantle Petrology: Field Observations and High Pressure Experimentation; a tribute to Francis R. (Joe) Boyd* (Y. Fei, C.M. Bertka and B.O. Mysen). Geochemical Society Special Publication No **6**.

Fei, Y., Mao, H.K. and Mysen, B.O. (1991) Experimental determination of element partitioning and calculation of phase relations in the MgO-FeO-SiO_2 system at high pressure and high temperature. *Journal of Geophysical Research*, **96**, 2157–2169.

Fei, Y., Wang, Y. and Finger, L.W. (1996) Maximum solubility of FeO in (Mg,Fe)SiO3-perovskite as a function of FeO content in the lower mantle. *Journal of Geophysical Research*, **101**, 11525–11530.

Frost, D.J. (2006) The stability of hydrous mantle phases. Pp. 243–271 in: *Water in Nominally Anhydrous Minerals* (H. Keppler and J.R. Smyth, editors). Reviews in Mineralogy and Geochemistry, **62**, Mineralogical Society of America, Chantilly, Virginia, USA.

Frost, D.J., Liebske, C., Langenhorst, F., McCammon, C.A., Trønnes, R.G. and Rubie, D.C. (2004) Experimental evidence for the existence of iron-rich metal in the Earth's lower mantle. *Nature*, **428**, 409–412.

Gasparik, T. and Hutchison, M.T. (2000) Experimental evidence for the origin of two kinds of inclusions in diamonds from the deep mantle. *Earth and Planetary*

Science Letters, **181**, 103–114.

Grevemeyer, I., Ranero, C.R., Flueh, E.R., Klaschen, D. and Bialas, J. (2007) Passive and active seismological study of bending-related faulting and mantle serpentinization at the Middle America trench. *Earth and Planetary Science Letters*, **258**, 528–542.

Griffin, W.L., Doyle, B.J., Ryan, C.G., Pearson, N.J., O'Reilly, S.Y., Davies, R.M., Kivi, K., Van Achterbergh, E. and Natapov, L.M. (1999) Layered mantle lithospherein the Lac de Gras area, Slave Craton: composition, structure and origin. *Journal of Petrology*, **40**, 705–727.

Gurney, J.J. (1989) Diamonds. Pp. 935–965 in: *Kimberlites and Related rocks, Vol.2: Their Mantle/Crust setting, Diamonds and Diamond Exploration* (J. Ross, editor). Geological Society of Australia, Special Publication No **14**.

Gurney, J.J., Harris, J.W., Rickard, R.S. and Moore, R.O. (1985) Premier mine diamond inclusions. *Transactions of the Geological Society of South Africa*, **88**, 301–310.

Haggerty, S.E. (1986) Diamond genesis in a multiply-constrained model. *Nature*, 320, 34–37.

Harlow, G.E. and Davies, R.M. (2005) Diamonds. *Elements*, **1**, 67–70.

Harris, J.W. (1987) Recent physical, chemical and isotopic research of diamond. Pp 478–500 in: *Mantle Xenoliths* (P.H. Nixon, editor). Wiley & Sons, London.

Harris, J.W. and Gurney, J.J. (1979) Inclusions in diamonds. Pp. 555–591 in: *Properties of Diamond* (J.E. Field, editor). Academic Press, London.

Harris, J.W., Hutchison, M.T., Hursthouse, M., Light, M. and Harte, B. (1997) A new tetragonal silicate mineral occurring as inclusions in lower mantle diamonds. *Nature*, **387**, 486–488.

Harte, B. (1992) Trace element characteristics of deep-seated eclogite parageneses – an ion microprobe study of inclusions in diamonds. Pp. A-48 in: *V.M. Goldschmidt Conference*, The Geochemical Society. Reston, Virginia, USA.

Harte, B. and Cayzer, N. (2007) Decompression and unmixing of crystals included in diamonds from the mantle transition zone. *Physics and Chemistry of Minerals*, **34**, 647–656.

Harte, B. and Hawkesworth, C.J. (1989) Mantle domains and mantle xenoliths. Pp. 649–686 in: *Kimberlites and Related rocks, Vol.2: Their Mantle/Crust Setting*, *Diamonds and Diamond Exploration* (J. Ross, editor). Geological Society of Australia, Special publication No **14**.

Harte, B., Fitzsimons, I.C.W., Harris, J.W. and Otter, M.L. (1999*a*) Carbon isotope ratios and nitrogen abundances in relation to cathodoluminescence characteristics for some diamonds from the Kaapvaal province, S. Africa. *Mineralogical Magazine*, **63**, 829–856.

Harte, B., Harris, J.W., Hutchison, M.T., Watt, G.R. and Wilding, M.C. (1999*b*) Lower mantle mineral associations in diamonds from Sao Luiz, Brazil. Pp. 125–153 in: *Mantle Petrology: Field Observations and High Pressure Experimentation; a tribute to Francis R. (Joe) Boyd* (Y. Fei, C.M. Bertka and B.O. Mysen, editors). The Geochemical Society Special Publication No **6**.

Hayman, P.C, Kopylova, M.G. and Kaminsky F.V. (2005) Lower Mantle Diamonds from Rio Soriso (Juina area, Mato Grosso, Brazil). *Contributions to Mineralogy and Petrology*, **149**, 430–445

Hirose, K. and Fei, Y. (2002) Subsolidus and melting relations of basaltic composition in the uppermost lower mantle. *Geochimica et Cosmochimica Acta*, **66**, 2099–2108.

Hirose, K., Fei, Y., Ono, S., Yagi, T. and Funakoshi, K. (2001) In situ measurements of the phase transition boundary in $Mg_3Al_2Si_3O_{12}$: implications for the nature of the seismic discontinuities in the Earth's mantle. *Earth and Planetary Science Letters*, **184**, 567–573.

Hirschmann, M.M., Aubaud, C. and Withers, A.C. (2005) Storage capacity of H_2O in nominally anhydrous minerals in the upper mantle. *Earth and Planetary Science Letters*, **236**, 167–181

Hutchison, M.T. (1997) *Constitution of the deep transition zone and lower mantle shown by diamonds and their inclusions.* PhD thesis, University of Edinburgh, Scotland, UK.

Hutchison, M.T., Cartigny, P. and Harris, J.W. (1999) Carbon and Nitrogen Compositons and Physical Characteristics of Transition zone and Lower mantle diamonds from São Luiz, Brazil. Pp. 372–382 in: *Proceedings of the VIIth International kimberlite Conference, J.B. Dawson volume* (J.J. Gurney, J.L. Gurney, M.D. Pascoe and S.H. Richardson, editors). Red Roof Design, Cape Town, RSA.

Hutchison, M.T., Hursthouse, M.B. and Light, M.E. (2001) Mineral inclusions in diamonds: associations and chemical distinctions around the 670 km discontinuity. *Contributions to Mineralogy and Petrology*, **142**, 119–126.

Inoue, T., Yurimoto, H. and Kudoh, Y. (1995) Hydrous modified spinel, $Mg_{1.75}SiH_{0.5}O_4$; a new water reservoir in the mantle transition region. *Geophysical Research Letters*, **22**, 117–120.

Irifune, T. (1987) An experimental investigation of the pyroxene-garnet transformation in a pyrolite composition and its bearing on the constitution of the mantle. *Physics of the Earth and Planetary Interiors*, **45**, 324–336.

Irifune, T. and Ringwood, A.E. (1987) Phase transformations in primitive MORB and pyrolite compositions to 25 GPa and some geophysical implications.

Pp. 231–242 in: *High Pressure Research in Geophysics* (Y. Manghnani and Y. Syono, editors). American Geophysical Union, Washington, D.C.

Irifune, T., Koizumi, T. and Ando, J-I. (1996) An experimental study of the garnet-perovskite transformation in the system $MgSiO_3$-$Mg_3Al_2Si_3O_{12}$. *Physics of the Earth and Planetary Interiors*, **96**, 147–157.

Ito, E. and Takahashi, E. (1989) Postspinel transformations in the system Mg_2SiO_4-Fe_2SiO_4 and some geophysical implications. *Journal of Geophysical Research*, **94**, 10637–10646.

Joswig, W., Stachel, T., Harris, J.W., Baur, W.H. and Brey, G.P. (1999) New Ca-silicate inclusions in diamonds – tracers from the lower mantle. *Earth and Planetary Science Letters*, **17**, 1–6.

Kaminsky, F.V., Zakharchenko, O.D., Davies, R., Griffin, W.L., Khacatryan-Blinova, G.K. and Shiryaev, A.A. (2001) Superdeep diamonds from the Juina area, Mato Grosso State, Brazil. *Contributions to Mineralogy and Petrology*, **140**, 734–753.

Kaminsky, F., Wirth, R. and Matsyuk, S. (2009) Carbonate and halide inclusions in diamond and deep-seated carbonatitic magma. *Geochimica et Cosmochimica Acta*, A1321.

Karato, S. (2006) Remote sensing of hydrogen in Earth's mantle. Pp. 343–375 in: *Water in nominally anhydrous minerals* (H. Keppler and J.R. Smyth, editors). Reviews in Mineralogy and Geochemistry, **62**, Mineralogical Society of America, Chantilly, Virginia, USA.

Kawamoto, T. (2006) Hydrous phases and water transport in the subducting slab. Pp. 273–289 in: *Water in Nominally Anhydrous Minerals* (H. Keppler and J.R. Smyth, editors). Reviews in Mineralogy and Geochemistry, **62**, Mineralogical Society of America, Chantilly, Virginia, USA.

King, D. (2007) In: *Mantle Dynamics* (D. Bercovici, editor). Elsevier, Amsterdam.

Kirkley, M.B., Gurney, J.J., Otter, M.L., Hill, S.J. and Daniels, L.R. (1991) The application of C isotope measurements to the identification of the sources of C in diamonds: a review. *Applied Geochemistry*, **6**, 477–494.

Komabayashi, T. (2006) Phase relations of hydrous peridotite: implications for water circulation in the Earth's mantle. Pp. 29–43 in: *Earth's Deep Water Cycle* (S. Jacobsen and S. van der Lee, editors). Monograph **168,** American Geophysical Union, Washington, D.C.

Komabayashi, T. and Omori, S. (2006) Internally consistent thermodynamic data set for dense hydrous magnesium silicates up to 35 GPa, 1600ºC: implications for water circulation in the Earth's deep mantle. *Physics of the Earth and Planetary Interiors*, **156**, 89–107.

Komabayashi, T., Omori, S. and Maruyama, S. (2004) Petrogenetic grid in the system MgO-SiO_2-H_2O up to 30 GPa, 1600ºC: applications to hydrous peridotite subducting into the Earth's deep interior. *Journal of Geophysical Research*, **109**, B03206.

Litvin, Yu.A, Litvin, V.Yu. and Kadik, A.A. (2008) Experimental characteristion of diamond crystallisation in melts of mantle silicate-carbonate-carbon systems at 7.0–8.5 GPa. *Geochemistry International*, **46**, 531–553.

McCammon, C.A., Stachel, T. and Harris, J.W. (2004) Iron oxidation state in lower mantle mineral assemblages II. Inclusions in diamonds from Kankan, Guinea. *Earth and Planetary Science Letters*, **222**, 423–434.

Moore, R.O. and Gurney, J.J. (1985) Pyroxene solid solution in garnets included in diamond. *Nature*, **318**, 553–555.

Moore, R.O. and Gurney, J.J. (1989) Mineral inclusions in diamonds from the Monastery kimberlite, South Africa. Pp. 1027–1041 in: *Kimberlites and Related rocks Vol.2: Their Mantle/Crust setting*, *Diamonds and Diamond Exploration* (J. Ross, editor). Geological Society of Australia Special Publication No. **14**.

Moore, R.O., Otter, M.L., Rickard, R.S., Harris, J.W. and Gurney, J.J. (1986) The occurrence of moisannite and ferro-periclase as inclusions in diamond. Pp. 409–411 in: *Fourth International Kimberlite Conference, Extended Abstracts* (C.B. Smith, editor). Geological Society of Australia Abstracts No. **16**.

Moore, R.O., Gurney, J.J., Griffin W.L. and Shimizu, N. (1991) Ultra-high pressure inclusions in Monastery diamonds: trace element abundance patterns and conditons of origin. *European Journal of Mineralogy*, **3**, 213–230.

Ohtani, E. (2005) Water in the mantle. *Elements*, **1**, 25–30.

Pearson, D.G., Canil, D. and Shirey, S.B. (2003) Mantle samples included in volcanic rocks: xenoliths and diamonds. Pp. 171–275 in: *The Mantle and Core (Treatise on Geochemistry)*. Amsterdam, Elsevier.

Perillat, J-P., Ricolleau, A., Daniel, I., Fiquet, G., Mezouar, M., Guignot, N. and Cardon, H. (2006) Phase transformations of subducted basaltic crust in the upmost lower mantle. *Physics of the Earth and Planetary Interiors*, **157**, 139–149.

Pokhilenko, N.P., Sobolev, N.V., Reutsky, V.N., Hall, A.E. and Taylor, L.A. (2004) Crystalline inclusions and C isotope ratios in diamonds from the Snap Lake/King Lake kimberlite dyke system: evidence of ultradeep and enriched lithospheric mantle. *Lithos*, **77**, 57–67.

Ringwood, A.E. (1991) Phase transformations and their

bearing on the constitution and dynamics of the mantle. *Geochimica et Cosmochimica Acta*, **55**, 2083–2110.

Ringwood, A.E. and Major, A. (1971) Synthesis of majorite and other high pressure garnets and perovskites. *Earth and Planetary Science Letters*, **12**, 411–418.

Schulze, D.J., Harte, B., Valley, J.W., Brenan, J.M. and Channer, D.M.De R. (2003) Extreme crustal oxygen isotope signatures preserved in coesite in diamond. *Nature*, **423**, 68–70.

Schulze, D.J., Harte, B., Valley, J.W. and Channer, D.M. DeR. (2004) Evidence of subduction and crust-mantle mixing from a single diamond. *Lithos*, **77**, 349–358.

Shirey, S.B., Richardson, S.H. and Harris, J.W. (2004) Integrated models of diamond formation and craton evolution. *Lithos*, **77**, 923–944.

Smyth, J.R. (1987) β-Mg_2SiO_4: a potential host for water in the mantle? *American Mineralogist*, **72**, 1051–1055.

Sobolev, N.V., Yefimova, E.S., Reimers, L.F., Zakharchenko, O.D., Makhin, A.I. and Usova, L.A. (1997) Mineral inclusions in diamonds of the Arkhangelsk kimberlite province. *Russian Geology and Geophysics*, **38**, 379–393.

Sobolev, N.V., Logvinova, A.M., Zedgenizov, D.A., Seryotkin, Y.V., Yefimova, E.S., Floss, C. and Taylor, L.A. (2004) Mineral inclusions in micro-diamonds and macrodiamonds from kimberlites of Yakutia: a comparative study. *Lithos*, **77**, 225–242.

Stachel, T. (2001) Diamonds from the asthenosphere and the transition zone. *European Journal of Mineralogy*, **13**, 883–892.

Stachel, T. and Harris, J.W. (2008) The origin of cratonic diamonds – constraints from mineral inclusions. *Ore Geology Reviews*, **34**, 5–32.

Stachel, T., Harris, J.W. and Brey, G.P. (1998) Rare and unusual mineral inclusions in diamonds from Mwadui, Tanzania. *Contributions to Mineralogy and Petrology*, **132**, 34–47.

Stachel, T., Brey, G.P. and Harris, J.W. (2000*a*) Kankan diamonds (Guinea) I: from lithosphere down to the Transition Zone. *Contributions to Mineralogy and Petrology*, **140**, 1–15.

Stachel, T., Harris, J.W., Brey, G.P. and Joswig, W. (2000*b*) Kankan diamonds (Guinea) II: lower mantle inclusion parageneses. *Contributions to Mineralogy and Petrology*, **140**, 16–27.

Stachel, T., Harris, J.W., Aulbach, S. and Deines, P. (2002) Kankan diamonds (Guinea) III: δ13 C and nitrogen characteristics of deep diamonds. *Contributions to Mineralogy and Petrology*, **142**, 465–475.

Stachel, T., Brey, G.P. and Harris, J.W. (2005) Inclusions in sublithospheric diamonds: glimpses of deep Earth. *Elements*, **1**, 73–78.

Stachel, T., Banas, A., Muelenbachs, K., Kurslaukis, S. and Walker, E.C. (2006) Archean diamonds from Wawa (Canada): samples from deep cratonic roots predating cratonization of the Superior Province. *Contributions to Mineralogy and Petrology*, **151**, 737–750.

Stixrude, L. and Lithgow-Bertelloni, C. (2007) Influence of phase transformations on lateral heterogeneity and dynamics in the Earth's mantle. *Earth and Planetary Science Letters*, **263**, 45–55.

Tappert, R., Stachel, T., Harris, J.W., Muelenbachs, K., Ludwig, T. and Brey, G.P. (2005*a*) Diamonds from Jagersfontein (South Africa): messengers from the sublithospheric mantle. *Contributions to Mineralogy and Petrology*, **150**, 505–522.

Tappert, R., Stachel, T., Harris, J.W., Muelenbachs, K., Ludwig, T. and Brey, G.P. (2005*b*) Subducting oceanic crust: The source of deep diamonds. *Geology*, **33**, 565–568.

Tappert, R., Stachel, T., Harris, J.W., Shimizu, N. and Brey, G.P. (2005*c*) Mineral Inclusions in diamonds from the Panda Kimberlite, Slave province, Canada. *European Journal of Mineralogy*, **17**, 423–440.

Tappert, R., Foden, J., Stachel, T., Muelenbachs, K., Tappert, M. and Wills, K. (2009*a*) Deep mantle diamonds from South Australia: A record of Pacific subduction at the Gondwanan margin. *Geology*, **37**, 43–46.

Tappert, R., Foden, J., Stachel, T., Muelenbachs, K., Tappert, M. and Wills, K. (2009*b*) The diamonds of South Australia. *Lithos*, **112**, 806–821.

Taylor, W.R. and Green, D.H. (1989) The role of reduced C-O-H fluids in mantle partial melting. Pp. 592–602 in: *Kimberlites and Related rocks, Vol. 1: Their Composition, Occurrence, Origin and Emplacement.* Geological Society of Australia, Special publication No **14**.

Torsvik, T., Furnes, H., Muehlenbachs, K., Thorseth, I.H. and Tumyr, O. (1998) Evidence for microbial activity at the glass-alteration interface in oceanic basalts. *Earth and Planetary Science Letters*, **162**, 103–114.

Walter, M.J., Bulanova, G.P., Armstrong, L.S., Keshav, S., Blundy, J.D., Gudfinnson, G., Lord, O.T., Lennie, A.R., Clark, S.M., Smith, C.B. and Gobbo, L. (2008) Primary carbonatite melt from deeply subducted oceanic crust. *Nature*, **454**, 622–626.

Wang, W. and Sueno, S. (1996) Discovery of a NaPx-En inclusion in diamond: possible transition zone origin. *Mineralogical Journal*, **18**, 9–16.

Wilding, M.C. (1990) *A study of diamonds with syngenetic inclusions*. PhD thesis, University of Edinburgh, Scotland, UK.

Wirth, R., Vollmer, C., Brenker, F., Matsyuk, S. and Kaminsky, F. (2007) Inclusions of nanocrystalline

aluminium silicate 'Phase Egg' in superdeep diamonds from Juina (Mato Grosso State, Brazil). *Earth and Planetary Science Letters*, **259**, 384–399.

Workman, R.K. and Hart, S.R. (2005) Major and trace element composition of the depleted MORB mantle (DMM). *Earth and Planetary Science Letters*, **231**, 53–72.